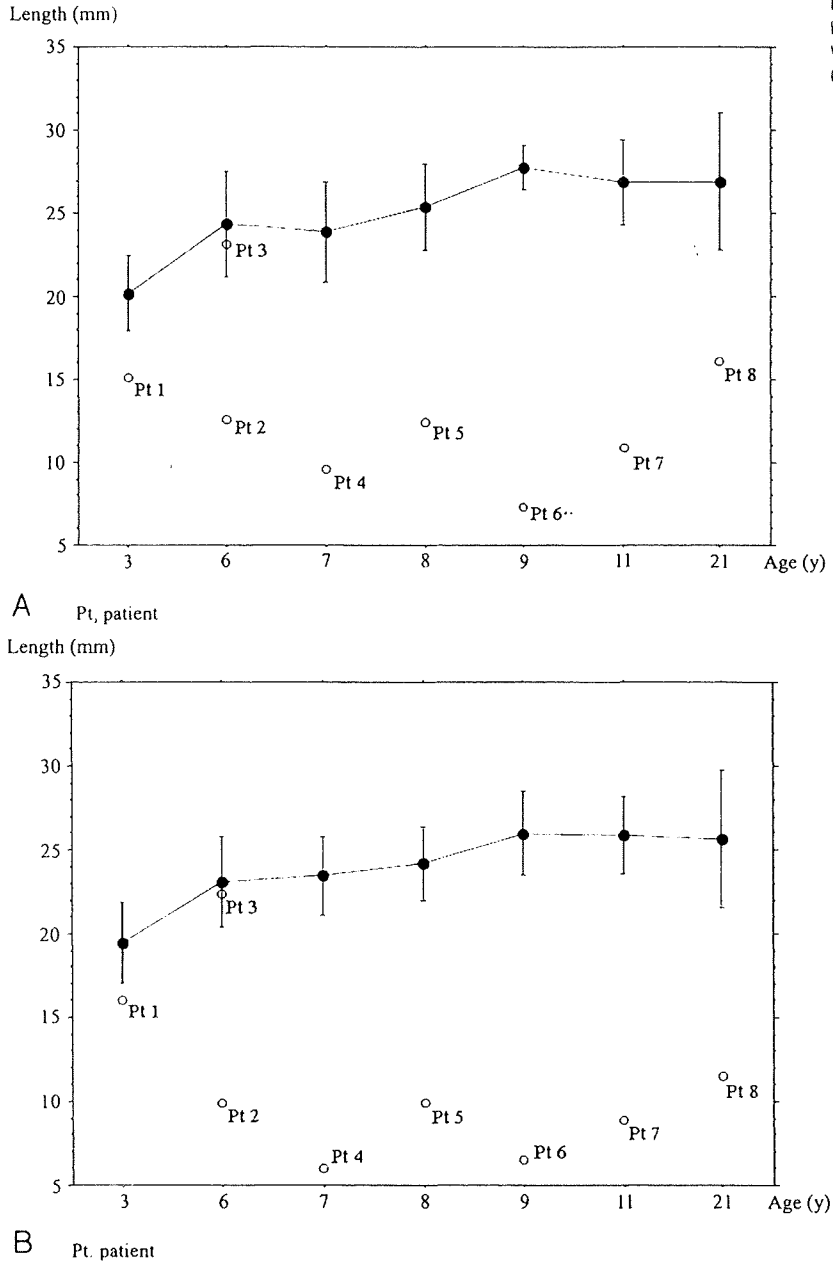

Fig 2. Line graph and bars show means and SDs of the length of Ba-Es (*A*) or Ba-Xs (*B*) for each age group of healthy controls. White dots show the length of Ba-Es or Ba-Xs of patients with CHARGE syndrome. Pt indicates patient.

Fig 3. T1-weighted sagittal images of patients 1 (*A*) and 4 (*B*). *A*, Mild hypoplastic basiocciput (*arrowhead*). *B*, Severe hypoplastic basiocciput (*arrowhead*) with basilar invagination and Chiari type I malformation (*arrow*).

and developmental pediatricians defined the major and minor criteria of CHARGE syndrome.[15] In the radiologic diagnostic methods, Chalouhi et al[11] reported that anomalies of the olfactory bulbs and tracts might be pathognomonic for

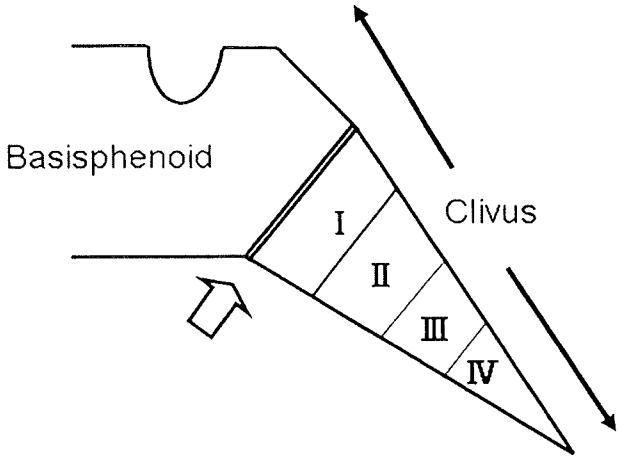

Fig 4. Contribution of the basiocciput, formed by 4 occipital sclerotomes (I-IV), to the lower portion of clivus. The upper potion is formed by the basisphenoid. The spheno-occipital synchondrosis (*open arrow*) lies in between.

CHARGE syndrome and should be included as a major criterion for the diagnosis of this syndrome; Blustajn et al[10] recently reported that these anomalies were the most prevalent features of CHARGE syndrome. The present study showed that basioccipital hypoplasia and basilar invagination are significantly prevalent in the syndrome. If our data are confirmed in a larger group of patients with CHARGE syndrome, these anomalies could serve as new criteria for the diagnosis. MR imaging enables simultaneous assessment of the semicircular canal, olfactory structures, and the basiocciput; and simultaneous detection of abnormalities involving these structures might enable us to make the imaging diagnosis of CHARGE syndrome.

Although the number of patients with this syndrome in the present study was small, basiocciput hypoplasia and basilar invagination were prevalent in our patients.

Conclusions

Basioccipital hypoplasia and basilar invagination are prevalent in patients with CHARGE syndrome. Routine assessment of the basiocciput in patients with CHARGE syndrome is helpful to exclude potentially life-threatening basilar invagination; identifica-
tion of these anomalies might help to accurately diagnose CHARGE syndrome.

References

1. Hall BD. **Choanal atresia and associated multiple anomalies.** *J Pediatr* 1979;95:395–98
2. Hittner HM, Hirsch NJ, Kreh GM, et al. **Colobomatous microphthalmia, heart disease, hearing loss, and mental retardation: a syndrome.** *J Pediatr Ophthalmol Strabismus* 1979;16:122–28
3. Pagon RA, Graham JM Jr, Zonana J, et al. **Coloboma, congenital heart disease, and choanal atresia with multiple anomalies: CHARGE association.** *J Pediatr* 1981;99:223–27
4. August GP, Rosenbaum KN, Friendly D, et al. **Hypopituitarism and the CHARGE association.** *J Pediatr* 1983;103:424–25
5. Lacombe D. **Facial palsy and cranial nerve abnormalities in CHARGE association.** *Am J Med Genet* 1994;49:351–53
6. Lin AE, Siebert JR, Graham JM Jr. **Central nervous system malformations in the CHARGE association.** *Am J Med Genet* 1990;37:304–10
7. Vissers LE, van Ravenswaaij CM, Admiraal R, et al. **Mutations in a new member of the chromodomain gene family cause CHARGE syndrome.** *Nat Genet* 2004; 36:955–57. Epub 2004 Aug 8
8. Jongmans MC, Admiraal RJ, van der Donk KP, et al. **CHARGE syndrome: the phenotypic spectrum of mutations in the CHD7 gene.** *J Med Genet* 2006;43:306–14
9. Lalani SR, Safiullah AM, Fernbach SD, et al. **Spectrum of CHD7 mutations in 110 individuals with CHARGE syndrome and genotype-phenotype correlation.** *Am J Hum Genet* 2006;78:303–14
10. Blustajn J, Kirsch CF, Panigrahy A, et al. **Olfactory anomalies in CHARGE syndrome: imaging findings of a potential major diagnostic criterion.** *AJNR Am J Neuroradiol* 2008;29:1266–69
11. Chalouhi C, Faulcon P, Le Bihan C, et al. **Olfactory evaluation in children: application to the CHARGE syndrome.** *Pediatrics* 2005;116:e81–88
12. Pinto G, Abadie V, Mesnage R, et al. **CHARGE syndrome includes hypogonadotropic hypogonadism and abnormal olfactory bulb development.** *J Clin Endocrinol Metabol* 2005;90:5621–26
13. Smoker WR. **Craniovertebral junction: normal anatomy, craniometry, and congenital anomalies.** *Radiographics* 1994;14:255–77
14. VanGilder JC, Menezes AH, Dolan KD. *The Craniovertebral Junction and Its Abnormalities.* New York: Furuta; 1987:113–18
15. Blake KD, Davenport SL, Hall BD, et al. **CHARGE association: an update and review for the primary pediatrician.** *Clin Pediatr (Phila)* 1998;37:159–73
16. Kosaki K, Suzuki T, Muroya K, et al. **PTPN11 (protein-tyrosine phosphatase, nonreceptor-type 11) mutations in seven Japanese patients with Noonan syndrome.** *J Clin Endocrinol Metabol* 2002;87:3529–33
17. Lang J, Issing P. **The measurements of the clivus, the foramina on the external base of the skull and the superior vertebrae** [in German]. *Anat Anz* 1989;169:7–34
18. Krompotić-Nemanić J, Vinter I, Kelovizc Z, et al. **Postnatal changes of the clivus.** *Ann Anat* 2005;187:277–80
19. Asakura Y, Toyota Y, Muroya K, et al. **Endocrine and radiological studies in patients with molecularly confirmed CHARGE syndrome.** *J Clin Endocrinol Metabol* 2008;93:920–24
20. Bassi P, Corona C, Contri P, et al. **Congenital basilar impression: correlated neurological syndromes.** *Eur Neurol* 1992;32:238–43
21. Paradis RW, Sax DS. **Familial basilar impression.** *Neurology* 1972;22:554–60
22. Bhangoo RS, Crockard HA. **Transmaxillary anterior decompressions in patients with severe basilar impression.** *Clin Orthop Relat Res* 1999;359:115–25
23. McAllion SJ, Paterson CR. **Causes of death in osteogenesis imperfecta.** *J Clin Pathol* 1996;49:627–30
24. Pozo JL, Crockard HA, Ransford AO. **Basilar impression in osteogenesis imperfecta: a report of three cases in one family.** *J Bone Joint Surg Br* 1984;66:233–38
25. Menezes AH. **Craniovertebral junction anomalies: diagnosis and management.** *Semin Pediatr Neurol* 1997;4:209–23
26. Bosman EA, Penn AC, Ambrose JC, et al. **Multiple mutations in mouse Chd7 provide models for CHARGE syndrome.** *Hum Mol Genet* 2005;14:3463–76. Epub 2005 Oct 5
27. Sanlaville D, Etchevers HC, Gonzales M, et al. **Phenotypic spectrum of CHARGE syndrome in fetuses with CHD7 truncating mutations correlates with expression during human development.** *J Med Genet* 2006;43:211–17
28. Nie X. **Cranial base in craniofacial development: developmental features, influence on facial growth, anomaly, and molecular basis.** *Acta Odontol Scand* 2005;63:127–35
29. Sandham A, Cheng L. **Cranial base and cleft lip and palate.** *Angle Orthod* 1988;58:163–68
30. Harris EF. **Size and form of the cranial base in isolated cleft lip and palate.** *Cleft Palate Craniofac J* 1993;30:170–74
31. Molsted K, Kjaer I, Dahl E. **Cranial base in newborns with complete cleft lip and palate: radiographic study.** *Cleft Palate Craniofac J* 1995;32:199–205

RESEARCH ARTICLE

AMERICAN JOURNAL OF medical genetics PART A

Characterization of the Complex 7q21.3 Rearrangement in a Patient With Bilateral Split-Foot Malformation and Hearing Loss

Hirotomo Saitsu,[1]* Kenji Kurosawa,[2] Hiroki Kawara,[3] Maki Eguchi,[3] Takeshi Mizuguchi,[1] Naoki Harada,[3] Tadashi Kaname,[4] Hiroki Kano,[5] Noriko Miyake,[1] Tatsushi Toda,[5] and Naomichi Matsumoto[1]

[1]Department of Human Genetics, Yokohama City University Graduate School of Medicine, Yokohama, Japan

[2]Division of Medical Genetics, Kanagawa Children's Medical Center, Yokohama, Japan

[3]Department of Molecular Cytogenetics, Kyushu Medical Science, Inc., Nagasaki, Japan

[4]Faculty of Medicine, Department of Medical Genetics, University of the Ryukyu, Okinawa, Japan

[5]Division of Clinical Genetics, Department of Medical Genetics, Osaka University Graduate School of Medicine, Suita, Japan

Received 3 August 2008; Accepted 9 March 2009

We report on complex rearrangements of the 7q21.3 region in a female patient with bilateral split-foot malformation and hearing loss. G-banding karyotype was 46,XX,t(7;15)(q21;q15), t(9;14)(q21;q11.2)dn. By fluorescence, in situ hybridization (FISH), Southern hybridization, and inverse PCR, the 7q21.3 translocation breakpoint was determined at the nucleotide level. The breakpoint did not disrupt any genes, but was mapped to 38-kb telomeric to the *DSS1* gene, and 258- and 272-kb centromeric to the *DLX6* and *DLX5* genes, respectively. It remains possible that the translocation would disrupt the interaction between these genes and their regulatory elements. Interestingly, microarray analysis also revealed an interstitial deletion close to (but not continuous to) the 7q21.3 breakpoint, indicating complex rearrangements within the split-hand/foot malformation 1 (*SHFM1*) locus in this patient. Furthermore, a 4.6-Mb deletion at 15q21.1-q21.2 adjacent to the 15q15 breakpoint was also identified. Cloning of the deletion junction at 7q21.3 revealed that the 0.8-Mb deletion was located 750-kb telomeric to the translocation breakpoint, encompassing *TACI*, *ASNS*, *OCM*, and a part of *LMTK2*. Because *TACI*, *ASNS*, and *OCM* genes were located on the reported copy number variation regions, it was less likely that the three genes were related to the split-foot malformation. *LMTK2* appeared to be a potential candidate gene for SHFM1, but no *LMTK2* mutations were found in 29 individuals with SHFM. Further *LMTK2* analysis of SHFM patients together with hearing loss is warranted. © 2009 Wiley-Liss, Inc.

Key words: split-hand/foot malformation; chromosomal translocation; deletion; 7q21.3; microarray

How to Cite this Article:
Saitsu H, Kurosawa K, Kawara H, Eguchi M, Mizuguchi T, Harada N, Kaname T, Kano H, Miyake N, Toda T, Matsumoto N. 2009. Characterization of the complex 7q21.3 rearrangement in a patient with bilateral split-foot malformation and hearing loss.
Am J Med Genet Part A 149A:1224–1230.

INTRODUCTION

Split-hand/foot malformation (SHFM) is a limb anomaly involving the central rays of the autopods, presenting with syndactyly, median clefts of hands and feet, and aplasia and/or hypoplasia of phalangeal, metacarpal and metatarsal bones. Five loci have been considered in relation to syndromic and non-syndromic SHFM: *SHFM1* on 7q21 [Scherer et al., 1994a], *SHFM2* on Xq26[Ahmad et al., 1987; Faiyaz-Ul-Haque et al., 2005], *SHFM3* on 10q24 [Nunes et al., 1995; Gurrieri et al., 1996; Raas-Rothschild et al., 1996], *SHFM4* on 3q27 [Celli et al., 1999; Ianakiev et al., 2000], and *SHFM5* on 2q31 [Boles et al., 1995; Goodman et al., 2002]. In addition, another locus on 8q21.1-q22.3 has been reported [Gurnett et al., 2006]. *TP63* was successfully isolated as a gene for *SHFM4*, but no other genes were identified from other loci [Celli et al., 1999; Ianakiev et al., 2000; van Bokhoven et al., 2001; Duijf et al., 2003]. Recently, homozygous *WNT10b* mutation at 12q13.12 has been reported in large consanguineous kindred with autosomal recessive SHFM [Ugur and Tolun, 2008].

Grant sponsor: Ministry of Health, Labour and Welfare; Grant sponsor: JST.

*Correspondence to:
Hirotomo Saitsu, Department of Human Genetics, Yokohama City University Graduate School of Medicine, Fukuura 3-9, Kanazawa-ku, Yokohama 236-0004, Japan. E-mail: hsaitsu@yokohama-cu.ac.jp

Published online 15 May 2009 in Wiley InterScience (www.interscience.wiley.com)
DOI 10.1002/ajmg.a.32877

The locus for SHFM1 (OMIM %183600) has been mapped to 7q21.3-q22.1 through the analysis of SHFM-associated chromosomal rearrangements [Scherer et al., 1994a; Crackower et al., 1996]. *DSS1*, *DLX5*, and *DLX6* genes within *SHFM1* have been suggested to be involved in pathogenesis of SHFM1 because of their roles in limb development in mice [Crackower et al., 1996; Robledo et al., 2002]. However, no gene mutations associated with SHFM1 have been reported to date [Crackower et al., 1996]. Hearing loss is commonly associated with SHFM1 (about 35%) [Elliott and Evans, 2006], and SHFM with sensorineural hearing loss, mapped to 7q21.2-q21.3, has been designated as a distinct (or overlapping) clinical entity (SHFM1D, OMIM %220600). Here we report on a patient with bilateral split-foot malformation as well as micrognathia, full lower lip, strabismus and stenosis of bilateral ear canals with a mixed (conductive and sensorioneural) type of hearing loss, and possessing a complex chromosomal rearrangement involving 7q21.3. Detailed genomic analysis of the 7q21.3 region implies a new candidate gene for SHFM1 with hearing loss.

MATERIALS AND METHODS

Clinical Report

The 9-year-old girl is a product of healthy and non-consanguineous parents. She was born at 38 weeks of gestation after uneventful pregnancy. Birth weight was 2,850 g (−0.02 SD), length 48 cm (−0.4 SD), and occipitofrontal circumference (OFC) was 32 cm (−0.5 SD). She was referred to us due to weak sucking at age of 1 month. Right foot showed cutaneous syndactyly of 4th and 5th digits, and absence of 2nd and 3rd digits. Only a reminiscent metatarsal was recognized in the position of 2nd and 3rd digits (Fig. 1A,B). Left foot showed cutaneous syndactyly of 1st and 2nd, and of 4th and 5th digits, and absence of 3rd digit. A defective metatarsal existed in the position of 3rd digit (Fig. 1A,C). Hands were normal by both clinical and radiographic appearance (data not shown). No family history of limb defects was noted. Micrognathia, full lower lip, strabismus, bilateral ear canal stenosis, and a severe mixed type of deafness (70 dB in right and 100 dB in left) were recognized. The strabismus was operated at 17 months, and a hearing aid was started at 14 months. Developmental milestones were delayed. She could walk alone at 21 months. Her development at 25 months was evaluated as an equivalent level at 7–8 months. Bilateral split-foot was surgically repaired at 39 months. Self-injuries, hyperactivity, and sleep disorders were observed since 3 years of age. At age of 8 years, her weight was 29.9 kg (+0.6 SD), height 133 cm (+1.1 SD), and OFC 52 cm (+0.2 SD).

Molecular Cytogenetic Analysis

G-banded chromosomes of peripheral lymphocytes and lymphoblastoid cell lines were analyzed. Fluorescence in situ hybridization (FISH) was performed using lymphoblastoid cell lines as previously described [Saitsu et al., 2008]. RPCI-11 BAC clones and approximately 10-kb probes amplified by long PCR using LA Taq polymerase (Takara Bio, Otsu, Japan) were used for FISH. Primer information is available on request.

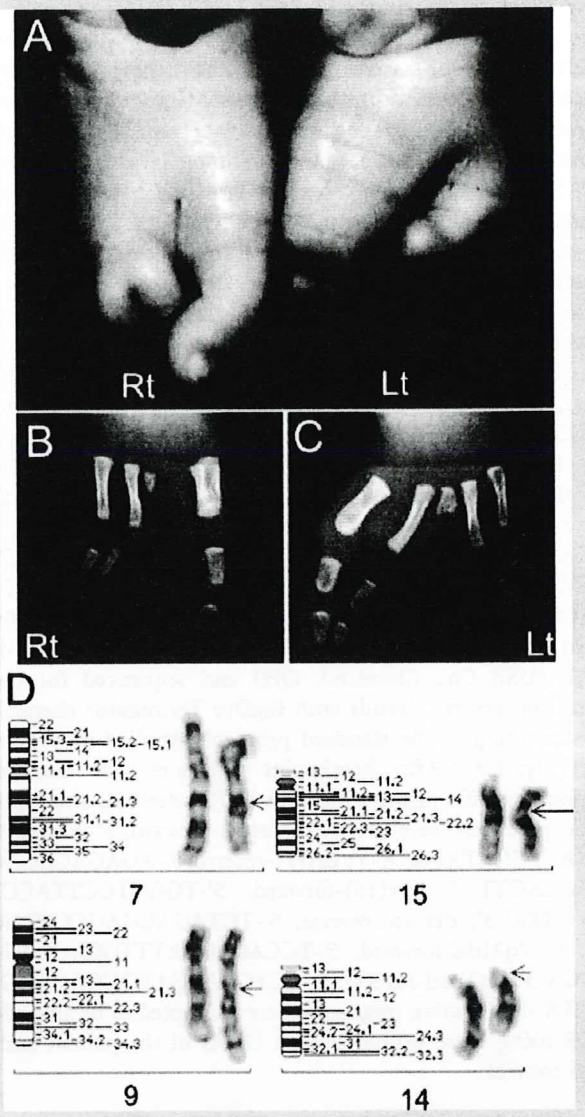

FIG. 1. The patient feet before surgical repair (A) and their X-ray images (B,C). Right foot showed cutaneous syndactyly of 4th and 5th digits, and absence of 2nd and 3rd digits. Only a reminiscent metatarsal was recognized in the position of 2nd and 3rd digits (A,B). Left foot showed cutaneous syndactyly of 1st and 2nd, and of 4th and 5th digits, and absence of 3rd digit. A defective metatarsal existed in the position of 3rd digit (A,C). Partial karyotype of the patient (D). Upper left figure shows chromosomes 7 (left: normal, right: derivative), upper right chromosomes 15 (left: normal, right: derivative), lower left chromosomes 9 (left: normal, right: derivative), and lower right chromosomes 14 (left: normal, right: derivative). Arrows indicate translocation breakpoints. Rt, right foot; Lt, left foot.

Cloning of Translocation and Deletion Breakpoints

The 7q21.3 translocation breakpoint was analyzed by Southern hybridization using *Eco*RI-, *Eco*RV-, *Bgl*II-, and *Nsi*I-digested patient DNA. Healthy female DNA was also used as a normal

control. Probes were synthesized by PCR DIG probe synthesis kit (Roche, Basel, Switzerland) using RP11-15f5 DNA as a template. Primer information is available on request. Hybridization, washing, and detection of probes were done according to the manufacturer's protocol. Images were captured on FluorChem (Alpha Innotech, San Leandro, CA). After identification of aberrant DNA fragments by Southern hybridization, size fractioning of electrophoresed *Eco*RI-, *Bgl*II-, and *Nsi*I-digested DNA of the patient was performed using QIAEXII Gel extraction kit (Qiagen, Valencia, CA) in order to obtain der(7), der(15), and 7q21.3 deletion junction fragments, respectively. The collected DNA was self-ligated by Ligation high (Toyobo, Osaka, Japan), ethanol precipitated, and dissolved in 20 μl EB buffer (Qiagen). Inverse PCR was performed in 25 μl of volume, containing 2 μl ligated DNA, 1× LA PCR bufferII, 2.5 mM $MgCl_2$, 0.4 mM each dNTP, 0.5 μM each primer, and 1.25 U LA Taq polymerase (Takara Bio). Primers were listed below: *Eco*RI-forward, 5′-TTTCCTCTTTCTCATAGGAAATGC-3′; *Eco*RI-reverse, 5′-ATGTTGGCAATCCGGTAGTC-3′; *Bgl*II-forward, 5′-CCTGTCTTGGGACTTTGAGG-3′; *Bgl*II-reverse, 5′-AACCAACCCTCTGGATGACA-3′; *Nsi*I-forward, 5′-AGGACCT-GGCCCTTGCTTTACACTT-3′; *Nsi*I-reverse, 5′-GGGCCCAACA-TAAAGCCCATCTCTA-3′. Negative controls only used either forward or reverse primer. The PCR product was purified with ExoSAP (USB Co., Cleveland, OH) and sequenced for both forward and reverse strands with BigDye Terminator chemistry ver. 3 according to the standard protocol (Applied Biosystems, Foster City, CA). After breakpoint sequences were disclosed, breakpoint-specific primers for both der(7), der(15), and 7q21.3 deletion junctions were designed: der(7)-forward, 5′-AAGAAG-CAAGATTGCCTATGAA-3′; der(7)-reverse, 5′-AGAGACAGAG-TCGGCCAGTT-3′; der(15)-forward, 5′-TGGGTCCTTACCT-TATGT-TGC-3′; der(15)-reverse, 5′-TCTAGAGGAGCGCTGG-CTAC-3′; 7q21del-forward, 5′-TCCACAGCATTTGCAGTAGA-ATCTGA-3′; 7q21del-reverse, 5′-GCTGAAAGATGGGAGAAGT-GGCCTA -3′. Junction fragments were attempted to be amplified by PCR using these primer-sets on DNAs of the patient and a normal control.

GeneChip Human Mapping 250K NspI Array

Genomic DNA obtained from peripheral blood leukocytes were used for microarray analysis. Experimental procedures were performed according to the manufacturer's protocol with slight modification (fragmentation time was shortened to 25 min). Call rate was 92.34%. Copy number alterations were analyzed by using CNAG2.0 [Nannya et al., 2005].

Quantitative Real-Time PCR

The interstitial deletion at 7q21.3 was analyzed using the patient's genomic DNA by quantitative real-time PCR (qPCR) on Rotor-Gene 6200 HRM (Corbett Life Science, Sydney, Australia). PCR was performed in a 10 μl of volume containing 10 ng genomic DNA, 1× ExTaq buffer, 0.2 mM each dNTP, 0.5 μM each primer, 0.25 μl LCGreen Plus (Idaho Technologies, Salt Lake City, UT) and 0.25 U Ex TaqHS polymerase (Takara Bio). Five sets of primers, including one normal control set on chromosome 15, were used as qPCR probes. The control set was assigned as a calibrator (a relative concentration of 1.00). The delta–delta C_t relative quantitative method was employed according to the manufacturer's protocol. Averages of duplicates were calculated by Rotor-Gene 6000 Series Software (Corbett Life Science). Primer information is available on request.

Mutation Analysis

LMTK2 was analyzed on a total of 29 Japanese patients with SHFM. One patient showed esophageal atresia and pulmonary atresia, and another showed tibial hemimelia. Among remaining 27 patients with non-syndromic SHFM (without any other anomalies), 25 patients showed no genomic rearrangement on 10q24 [Kano et al., 2005]. The other four patients have not been analyzed for the 10q24 rearrangement. No patient had hearing loss. Genomic DNA was obtained from peripheral blood leukocytes according to standard protocols. Genomic DNA was amplified using Genomiphi version 2 (GE Healthcare, Buckinghamshire, UK), and then used for mutation analysis. Mutation of 1st to 14th exons covering the *LMTK2* coding region was screened by high-resolution melt analysis. Real-time PCR and subsequent high-resolution melt analysis were performed in 12-μl mixture on RoterGene-6200HRM (Corbett Life Science) as previously described [Saitsu et al., 2008]. PCR conditions and primer sequences are available on request.

RESULTS

G-banded chromosomal analysis revealed double balanced translocations. The karyotype was 46,XX,t(7;15)(q21;q15),t(9;14)-(q21;q11.2) (Fig. 1D). Her parents showed a normal karyotype (data not shown). To check genomic copy number alterations accompanied by translocations, GeneChip Human Mapping 250K NspI (Affymetrix, Santa Clara, CA) was performed. A ~1-Mb interstitial deletion at 7q21.3 and an approximately 4.6-Mb deletion at 15q21.1-q21.2 were found (Fig. 2A, arrow and Fig. 3, bidirectional arrow). No other abnormal copy number alterations were not found around the 9q21 and 14q11.2 regions (data not shown).

Because the patient showed SHFM with hearing loss, we first analyzed chromosomal rearrangement of the 7q21.3 region (Fig. 2A). By FISH analysis using BAC clones around at 7q21, RP11 -15f5 [UCSC genome browser coordinate (version Mar. 2006): chr7:96, 097, 195–96, 276, 197 bp] was found to span the 7q21 breakpoint as its signals were recognized on der(7), der(15), and normal chromosome 7 (Fig. 2A,B). The breakpoint was further narrowed down by FISH analysis using long PCR products as probes (Fig. 2A,B). While probe I showed only two signals, probe II showed split signals (three signals) in the patient's interphase nuclei, indicating that the breakpoint was located within probe II (Fig. 2A,B). The 7q21.3 deletion junction was narrowed down by qPCR (Fig. 2A).

Southern hybridization analysis using probes P1, P2, and P3 detected aberrant bands (Fig. 2A,C). Inverse PCR on *Eco*RI-, *Bgl*II-, and *Nsi*I-digested DNA was successful for obtaining der(7), der(15), and 7q21.3 deletion junction fragments, respectively. Sequence analysis showed that the 7q21.3 translocation breakpoint was located 38 kb telomeric to *DSS1*, and 258- and 272-kb centro-

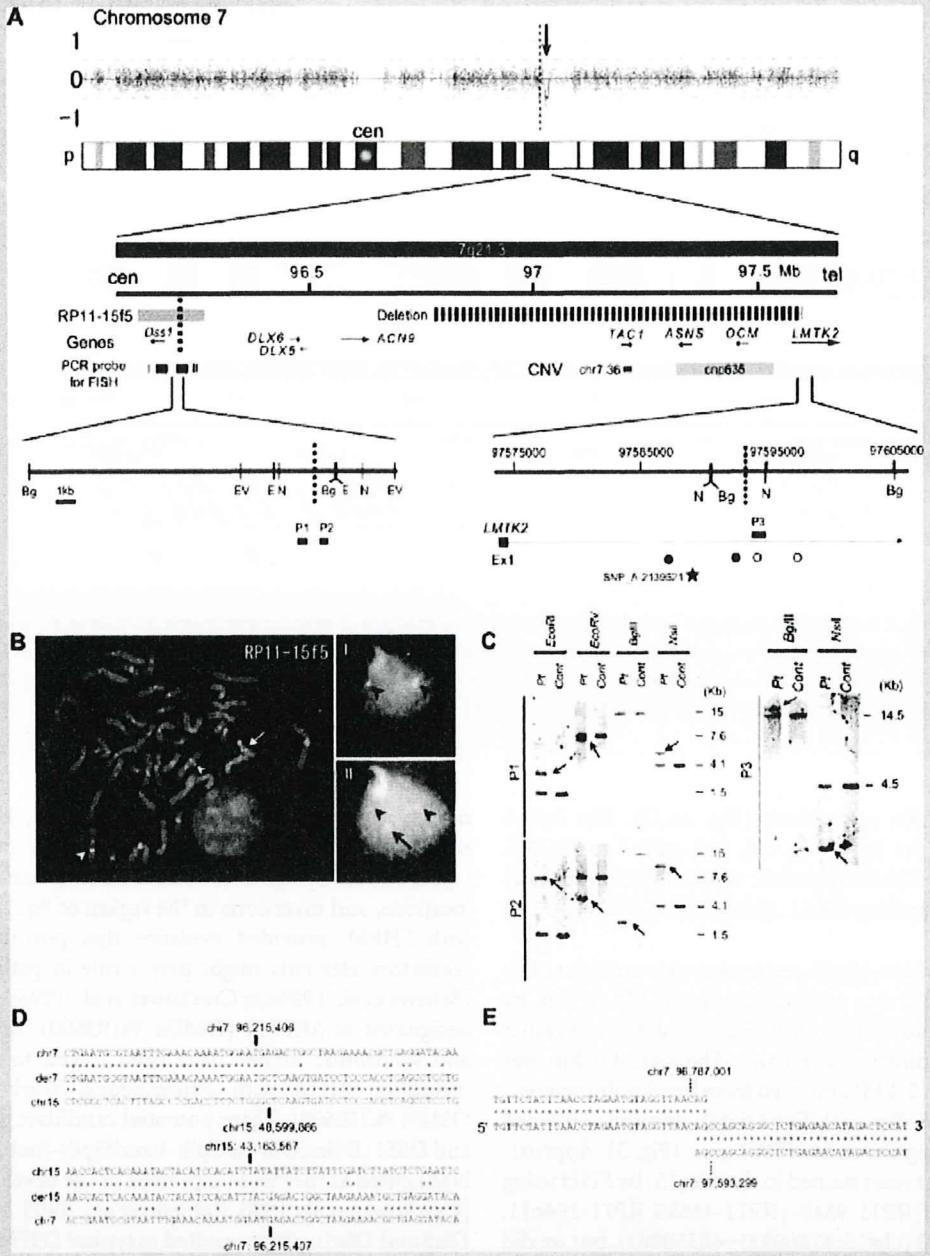

FIG. 2. Characterization of the 7q21.3 rearrangement. A: GeneChip analysis of chromosomes 7 in the patient (top). The position (*x* axis matching the chromosomal 7 ideogram) and log2 (signal ratio) values (*y* axis) of each SNP probes are indicated. A thin line indicates copy number inference from Hidden Markov Model. An interstitial deletion at 7q21.3 (arrow) was identified apart from 7q21.3 breakpoint (dashed line). The 7q21.3 genomic rearrangement is schematically presented (middle). RP11-15f5 and PCR probe II span the translocation breakpoint (dashed line). The deletion (dashed thick line) encompasses four genes. *TAC1*, *ASNS*, and *OCM* are overlapped with reported copy number variation (CNV) regions (chr7.36 and cnp635). More detailed maps are shown (bottom). Restriction sites (E, *Eco*RI; EV, *Eco*RV; Bg, *Bgl*II; N, *Nsi*I) and probes for Southern hybridization (P1-3) are indicated. Translocation breakpoint (dashed line) is located between P1 and P2, and distal deletion breakpoint (dashed line) is flanked by P3. A probe (SNP_A-2139521) in GeneChip (filled star, deleted), positions for qPCR primer-sets (filled circle, deleted; open circle, not deleted) are also depicted. B: FISH analysis using a clone (RP11-15f5) and two long PCR probes (I and II in A) on the patient's metaphase chromosomes or interphase nuclei. Arrowhead indicates a signal on chromosomes 7 and arrow shows a signal on a derivative chromosome 15, indicating RP11-15f5 and probe II span the breakpoint. C: Southern hybridization using probes P1, P2, and P3 on the patient's genomic DNA. Arrow shows aberrant bands specific to the patient (not observed in control DNA). D: Breakpoint junction sequences of der(7) and der(15). In upper part, top, middle, and bottom sequence strands show chromosome 7, derivative chromosome 7, and chromosome 15 sequences, respectively. In lower part, top, middle, and bottom strands show chromosome 15, derivative chromosome 15, and chromosome 7 sequences, respectively. Breakpoint positions are marked according to the UCSC genome browser coordinate (version Mar. 2006). Asterisks indicate nucleotides identical to normal chromosomes. E: Deletion junction sequence. Top, middle, and bottom strands show proximal, recombined, and distal sequences, respectively. Deletion breakpoint location is marked. Two nucleotides were overlapped. Asterisks are matched nucleotides in chromosome 7 sequence.

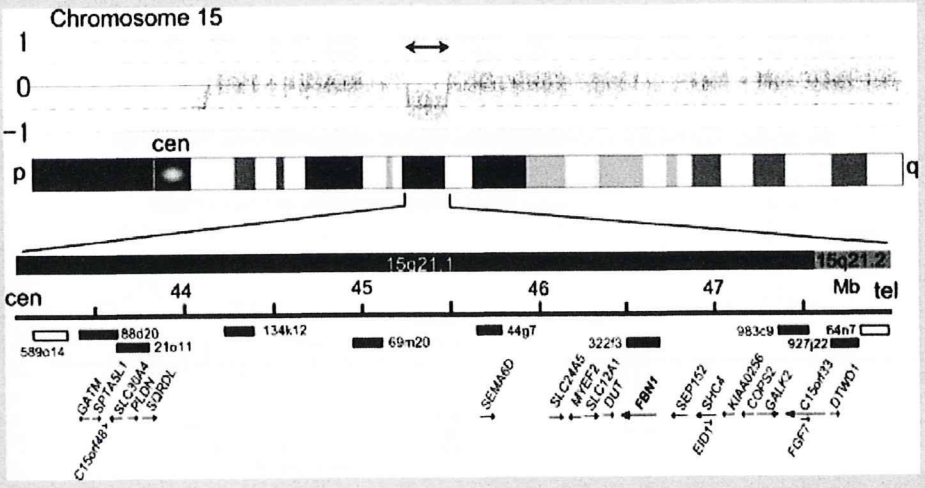

FIG. 3. Characterization of the 15q21 rearrangement. Upper panel: GeneChip analysis of entire chromosome 15 clearly shows the deletion (bidirectional arrow). Deletion at 15q11.2 is reported as a copy number variation. Lower panel: A genomic map of the 15q21.1-q21.2 deletion with 4.6 Mb in size is shown with position of BAC clones used for FISH. Black and white indicates deleted and intact (not deleted), respectively. A total of 21 RefSeq genes, including *FBN1*, are mapped within the deletion (bottom).

meric to *DLX6* and *DLX5*, respectively (Fig. 2A,D). The 7q21.3 deletion was 806 kb in size (from chr7:96, 215, 406–7 to 97, 593, 297–9) and was located 750-kb telomeric to the 7q21.3 translocation breakpoint, encompassing *TAC1*, *ASNS*, *OCM*, and exon 1 of *LMTK2* (Fig. 2A,E).

The rearrangement of the 15q21 region was also complex. The deletion at 15q21.1-q21.2 was approximately 4.6 Mb in size by Affymetrix GeneChip and further BAC FISH analysis, but rather complicated (Fig. 3, bidirectional arrow). The size, 4.6 Mb was somehow different from 5.4 Mb, inferred from breakpoint sequences of der(7) and der(15) (Fig. 2D). The 4.6-Mb deletion contained 21 RefSeq genes including the entire *FBN1* gene (Fig. 3). Approximately a 0.7-Mb segment was retained in the der(15) by FISH using RP11-64n7, RP11-112e7, RP11-964b7, RP11-416k5, RP11-294o11, and partial RP11-637h23 (chr15: 47869993–48550883), but we did not further investigate the retained segment as our main focus was the 7q21.3 region. The rearrangement junctions from both of derivative chromosomes were successfully amplified by PCR only on the patient DNA (data not shown).

We hypothesized that a gene(s) in the 806-kb deletion at 7q21.3 could be responsible for the split-foot phenotype. As *TAC1*, *ASNS*, and *OCM* were overlapped with reported copy number variation regions (chr7.36 and cnp635 in the database; Fig. 2A), it was less likely that a heterozygous deletion of these genes would cause the split-foot phenotype. *LMTK2* gene appeared to be a candidate for SHFM1. We performed *LMTK2* mutation screening in 29 SHFM patients without hearing loss, but no pathological mutations were found.

DISCUSSION

SHFM is a human developmental disorder characterized by missing central rays of the distal extremities, including phalangeal, metacarpal, and metatarsal bones [Elliott et al., 2005]. SHFM occur either isolated (non-syndromic) or with other abnormalities (syndromic). Cytogenetic abnormalities, such as deletions, translocations, and inversions in the region of 7q21.3-q22.1 in patients with SHFM, provided evidence that positional effects and/or regulatory elements might play a role in pathogenesis of SHFM [Scherer et al., 1994a,b; Crackower et al., 1996]. This locus has been designated as *SHFM1* (OMIM %183600). Both non-syndromic and syndromic SHFM have been linked to the *SHFM1* locus, including SHFM with sensorineural hearing loss (SHFM1D; OMIM %220600). Three potential candidate genes, *DLX5*, *DLX6*, and *DSS1* (Deleted in the Split-hand/Split-foot 1 region), have been highlighted as they were expressed in the developing limbs in mice [Crackower et al., 1996; Robledo et al., 2002]. Double knockout of *Dlx5* and *Dlx6* in mice resulted in typical SHFM as well as inner ear and severe craniofacial defects [Robledo et al., 2002]. However, the three candidate genes did not seem to be interrupted directly by any of human chromosomal rearrangements, and did not show any point mutations in SHFM patients [Crackower et al., 1996]. One possible hypothesis is that disruption of distant cis-acting regulatory elements or positional effects results in aberrant expression of *DSS1*, *DLX5*, and *DLX6* leading to SHFM1 [Crackower et al., 1996; Scherer et al., 2003]. Alternatively, a gene, not yet identified, exists in different region of SHFM1. *TP63*, encoding P63, is the gene identified in both syndromic and non-syndromic SHFM [Celli et al., 1999; Ianakiev et al., 2000; van Bokhoven et al., 2001; Duijf et al., 2003]. Recently, *p63* has been shown to directly regulate expression of *Dlx5* and *Dlx6* in apical ectodermal ridge in mice [Lo Iacono et al., 2008], suggesting that *p63* and the *Dlx5/Dlx6* locus are involved in the same pathway of SHFM pathogenesis.

Here we report on an unexpected 806 kb interstitial deletion together with a chromosomal translocation in the *SHFM1* locus of the patient with SHFM1D. The deletion involved *TAC1*, *ASNS*,

OCM, and *LMTK2* and we considered *LMTK2* worthy of attention. LMTK2 is a transmembrane protein which possesses serine/threonine kinase activity [Wang and Brautigan, 2002]. It is expressed predominantly in skeletal muscle [Wang and Brautigan, 2002]. The knockout mouse showed no limb abnormalities but azoospermia [Kawa et al., 2006]. As no *LMTK2* mutations were observed in 29 SHFM patients without hearing loss, it may be interesting to investigate *LMTK2* mutations particularly in SHFM1D.

The 4.6-Mb deletion at 15q21.1-q21.2 encompassed 21 RefSeq genes. We could not exclude the possibility that the deletion of these genes may contribute to the patient's phenotype including SHFM, though any known SHFM loci are not associated with 15q21. It should be noted that *FBN1* was completely deleted. Haploinsufficiency of *FBN1* could be involved in pathogenesis of Marfan syndrome [Mizuguchi and Matsumoto, 2007], but the patient did not show any Marfan syndrome features.

In conclusion, the complex 7q21.3 rearrangement in the SHFM1D patient was intensively analyzed. Microarray analysis may potentially add novel findings leading to full understanding of SHFM1D and/or SHFM.

ACKNOWLEDGMENTS

We thank patients and their families for their participation in this study. This study was supported by a research grant from the Ministry of Health, Labour and Welfare (N.M.) and SORST from JST (N.M.).

REFERENCES

Ahmad M, Abbas H, Haque S, Flatz G. 1987. X-chromosomally inherited split-hand/split-foot anomaly in a Pakistani kindred. Hum Genet 75: 169–173.

Boles RG, Pober BR, Gibson LH, Willis CR, McGrath J, Roberts DJ, Yang-Feng TL. 1995. Deletion of chromosome 2q24-q31 causes characteristic digital anomalies: Case report and review. Am J Med Genet 55:155–160.

Celli J, Duijf P, Hamel BC, Bamshad M, Kramer B, Smits AP, Newbury-Ecob R, Hennekam RC, Van Buggenhout G, van Haeringen A, Woods CG, van Essen AJ, de Waal R, Vriend G, Haber DA, Yang A, McKeon F, Brunner HG, van Bokhoven H. 1999. Heterozygous germline mutations in the p53 homolog p63 are the cause of EEC syndrome. Cell 99:143–153.

Crackower MA, Scherer SW, Rommens JM, Hui CC, Poorkaj P, Soder S, Cobben JM, Hudgins L, Evans JP, Tsui LC. 1996. Characterization of the split hand/split foot malformation locus SHFM1 at 7q21.3-q22.1 and analysis of a candidate gene for its expression during limb development. Hum Mol Genet 5:571–579.

Duijf PHG, van Bokhoven H, Brunner HG. 2003. Pathogenesis of split-hand/split-foot malformation. Hum Mol Genet 12:R51–R60.

Elliott AM, Evans JA. 2006. Genotype-phenotype correlations in mapped split hand foot malformation (SHFM) patients. Am J Med Genet Part A 140A:1419–1427.

Elliott AM, Evans JA, Chudley AE. 2005. Split hand foot malformation (SHFM). Clin Genet 68:501–505.

Faiyaz-Ul-Haque M, Zaidi SH, King LM, Haque S, Patel M, Ahmad M, Siddique T, Ahmad W, Tsui LC, Cohn DH. 2005. Fine mapping of the X-linked split-hand/split-foot malformation (SHFM2) locus to a 5.1-Mb region on Xq26.3 and analysis of candidate genes. Clin Genet 67: 93–97.

Goodman FR, Majewski F, Collins AL, Scambler PJ. 2002. A 117-kb microdeletion removing HOXD9-HOXD13 and EVX2 causes synpolydactyly. Am J Hum Genet 70:547–555.

Gurnett CA, Dobbs MB, Nordsieck EJ, Keppel C, Goldfarb CA, Morcuende JA, Bowcock AM. 2006. Evidence for an additional locus for split hand/foot malformation in chromosome region 8q21.11-q22.3. Am J Med Genet Part A 140A:1744–1748.

Gurrieri F, Prinos P, Tackels D, Kilpatrick MW, Allanson J, Genuardi M, Vuckov A, Nanni L, Sangiorgi E, Garofalo G, Nunes ME, Neri G, Schwartz C, Tsipouras P. 1996. A split hand-split foot (SHFM3) gene is located at 10q24–>25. Am J Med Genet 62:427–436.

Ianakiev P, Kilpatrick MW, Toudjarska I, Basel D, Beighton P, Tsipouras P. 2000. Split-hand/split-foot malformation is caused by mutations in the p63 gene on 3q27. Am J Hum Genet 67:59–66.

Kano H, Kurosawa K, Horii E, Ikegawa S, Yoshikawa H, Kurahashi H, Toda T. 2005. Genomic rearrangement at 10q24 in non-syndromic split-hand/split-foot malformation. Hum Genet 118:477–483.

Kawa S, Ito C, Toyama Y, Maekawa M, Tezuka T, Nakamura T, Nakazawa T, Yokoyama K, Yoshida N, Toshimori K, Yamamoto T. 2006. Azoospermia in mice with targeted disruption of the Brek/Lmtk2 (brain-enriched kinase/lemur tyrosine kinase 2) gene. Proc Natl Acad Sci 103:19344–19349.

Lo Iacono N, Mantero S, Chiarelli A, Garcia E, Mills AA, Morasso MI, Costanzo A, Levi G, Guerrini L, Merlo GR, 2008. Regulation of Dlx5 and Dlx6 gene expression by p63 is involved in EEC and SHFM congenital limb defects. Development 135:1377–1388.

Mizuguchi T, Matsumoto N. 2007. Recent progress in genetics of Marfan syndrome and Marfan-associated disorders. J Hum Genet 52:1–12.

Nannya Y, Sanada M, Nakazaki K, Hosoya N, Wang L, Hangaishi A, Kurokawa M, Chiba S, Bailey DK, Kennedy GC, Ogawa S. 2005. A robust algorithm for copy number detection using high-density oligonucleotide single nucleotide polymorphism genotyping arrays. Cancer Res 65: 6071–6079.

Nunes ME, Schutt G, Kapur RP, Luthardt F, Kukolich M, Byers P, Evans JP. 1995. A second autosomal split hand/split foot locus maps to chromosome 10q24-q25. Hum Mol Genet 4:2165–2170.

Raas-Rothschild A, Manouvrier S, Gonzales M, Farriaux JP, Lyonnet S, Munnich A. 1996. Refined mapping of a gene for split hand-split foot malformation (SHFM3) on chromosome 10q25. J Med Genet 33: 996–1001.

Robledo RF, Rajan L, Li X, Lufkin T. 2002. The Dlx5 and Dlx6 homeobox genes are essential for craniofacial, axial, and appendicular skeletal development. Genes Dev 16:1089–1101.

Saitsu H, Kato M, Mizuguchi T, Hamada K, Osaka H, Tohyama J, Uruno K, Kumada S, Nishiyama K, Nishimura A, Okada I, Yoshimura Y, Hirai S, Kumada T, Hayasaka K, Fukuda A, Ogata K, Matsumoto N. 2008. De novo mutations in the gene encoding STXBP1 (MUNC18–1) cause early infantile epileptic encephalopathy. Nat Genet 40:782–788.

Scherer SW, Poorkaj P, Allen T, Kim J, Geshuri D, Nunes M, Soder S, Stephens K, Pagon RA, Patton MA, et al. 1994a. Fine mapping of the autosomal dominant split hand/split foot locus on chromosome 7, band q21.3-q22.1. Am J Hum Genet 55:12–20.

Scherer SW, Poorkaj P, Massa H, Soder S, Allen T, Nunes M, Geshuri D, Wong E, Belloni E, Little S, et al. 1994b. Physical mapping of the split hand/split foot locus on chromosome 7 and implication in syndromic ectrodactyly. Hum Mol Genet 3:1345–1354.

Scherer SW, Cheung J, MacDonald JR, Osborne LR, Nakabayashi K, Herbrick JA, Carson AR, Parker-Katiraee L, Skaug J, Khaja R, Zhang

J, Hudek AK, Li M, Haddad M, Duggan GE, Fernandez BA, Kanematsu E, Gentles S, Christopoulos CC, Choufani S, Kwasnicka D, Zheng XH, Lai Z, Nusskern D, Zhang Q, Gu Z, Lu F, Zeesman S, Nowaczyk MJ, Teshima I, Chitayat D, Shuman C, Weksberg R, Zackai EH, Grebe TA, Cox SR, Kirkpatrick SJ, Rahman N, Friedman JM, Heng HH, Pelicci PG, Lo-Coco F, Belloni E, Shaffer LG, Pober B, Morton CC, Gusella JF, Bruns GA, Korf BR, Quade BJ, Ligon AH, Ferguson H, Higgins AW, Leach NT, Herrick SR, Lemyre E, Farra CG, Kim HG, Summers AM, Gripp KW, Roberts W, Szatmari P, Winsor EJ, Grzeschik KH, Teebi A, Minassian BA, Kere J, Armengol L, Pujana MA, Estivill X, Wilson MD, Koop BF, Tosi S, Moore GE, Boright AP, Zlotorynski E, Kerem B, Kroisel PM, Petek E, Oscier DG, Mould SJ, Dohner H, Dohner K, Rommens JM, Vincent JB, Venter JC, Li PW, Mural RJ, Adams MD, Tsui LC. 2003. Human chromosome 7: DNA sequence and biology. Science 300: 767–772.

Ugur SA, Tolun A. 2008. Homozygous WNT10b mutation and complex inheritance in split hand foot malformation. Hum Mol Genet 17: 2644–2653.

van Bokhoven H, Hamel BC, Bamshad M, Sangiorgi E, Gurrieri F, Duijf PH, Vanmolkot KR, van Beusekom E, van Beersum SE, Celli J, Merkx GF, Tenconi R, Fryns JP, Verloes A, Newbury-Ecob RA, Raas-Rotschild A, Majewski F, Beemer FA, Janecke A, Chitayat D, Crisponi G, Kayserili H, Yates JR, Neri G, Brunner HG. 2001. p63 Gene mutations in eec syndrome, limb-mammary syndrome, and isolated split hand-split foot malformation suggest a genotype-phenotype correlation. Am J Hum Genet 69:481–492.

Wang H, Brautigan DL. 2002. A Novel transmembrane Ser/Thr kinase complexes with protein phosphatase-1 and inhibitor-2. J Biol Chem 277:49605–49612.

 doi:10.1111/j.1741-4520.2008.00212.x

ORIGINAL ARTICLE

Further delineation of 9q22 deletion syndrome associated with basal cell nevus (Gorlin) syndrome: Report of two cases and review of the literature

Kayono Yamamoto[1,2]*, Hiroshi Yoshihashi[2]*, Noritaka Furuya[2], Masanori Adachi[3], Susumu Ito[4], Yukichi Tanaka[5], Mitsuo Masuno[2], Hideaki Chiyo[1], and Kenji Kurosawa[2]

[1]Department of Genetic Counseling, Graduate School of Humanities and Sciences, Ochanomizu University, Tokyo, and Divisions of [2]Medical Genetics, [3]Endocrinology and Metabolism, [4]Neurosurgery and [5]Pathology, Kanagawa Children's Medical Center, Yokohama, Japan

ABSTRACT **Basal cell nevus syndrome (BCNS; Gorlin syndrome) is an autosomal dominant disorder, characterized by a predisposition to neoplasms and developmental abnormalities. BCNS is caused by mutations in the human homolog of the *Drosophila* patched gene-1, *PTCH1*, which is mapped on chromosome 9q22.3. Nonsense, frameshift, in-frame deletions, splice-site, and missense mutations have been found in the syndrome. Haploinsufficiency of *PTCH1*, which is caused by interstitial deletion of 9q22.3, is also responsible for the syndrome. To date, 19 cases with interstitial deletion of long arm of chromosome 9 involving the region of q22 have been reported. We describe two unrelated patients with some typical features of BCNS associated with deletion of 9q21.33-q31.1 and determined the boundary of the deletion by fluorescence *in situ* hybridization (FISH) with bacterial artificial chromosome (BAC) clones. The results showed that the size of deletions is between 15.33 and 16.04 Mb in patient 1 and between 18.08 and 18.54 Mb in patient 2. Although the size and breakpoints were different from those of previously reported cases, the clinical features are common to patients with 9q22 deletion associated with BCNS. Delineation of the 9q22 deletions and further consideration of the genes responsible for the characteristic manifestations may provide insight into this newly recognized deletion syndrome.**

Key Words: basal cell nevus syndrome, chromosome deletion syndrome, FISH, Gorlin syndrome, *PTCH1*

INTRODUCTION

Basal cell nevus syndrome (BCNS, OMIM# 109400), also known as Gorlin syndrome, is an autosomal dominant disorder characterized by a predisposition to neoplasms and developmental abnormalities. The cardinal features include an excess of multiple basal cell carcinoma, odontogenic keratocysts, palmar and plantar epidermal pits, calcification of the falx cerebri, spine and rib anomalies, relative macrocephaly, frontal bossing, facial milia, ocular malformation, medulloblastomas, cleft lip and/or palate, and developmental malformations (Gorlin & Goltz 1960). The prevalence of BCNS has been estimated to be from 1 in 57 000 to 1 in 164 000 (Evans *et al.* 1991). BCNS is caused by mutations in the human homolog of the *Drosophila* patched-1 gene, *PTCH1*. *PTCH1* is mapped on chromosome 9q22.3, contains 24 exons spanning approximately 50 kb, and encodes a 1447-amino acid transmembrane glycoprotein (Hahn *et al.* 1996; Johnson *et al.* 1996). Nonsense, frameshift, in-frame deletions, splice-site, and missense mutations have been found in the syndrome. Furthermore, haploinsufficiency of *PTCH1*, which is caused by interstitial deletion of 9q22.3, is responsible for the syndrome. Compared to the germline mutations, *PTCH1* mutations are also found in many sporadic tumors, such as medulloblastomas, squamous cell carcinomas, breast cancer, and colon cancer (Lindström *et al.* 2006). There have been few recurrent mutations and no genotype-phenotype correlations (Wicking *et al.* 1997). The loss of heterozygosity of the 9q chromosomal region suggested that *PTCH1* acts as a classic tumor suppressor gene (Hahn *et al.* 1996).

To date, 19 cases with interstitial deletion of long arm of chromosome 9 involving the region of q22 have been reported (Ying *et al.* 1982; Farrell *et al.* 1991; Robb *et al.* 1991; Kroes *et al.* 1994; Shimkets *et al.* 1996; Sasaki *et al.* 2000; Olivieri *et al.* 2003; Haniffa *et al.* 2004; Midro *et al.* 2004; Boonen *et al.* 2005; Chen *et al.* 2006; Redon *et al.* 2006; Soufir *et al.* 2006; Fujii *et al.* 2007; Nowakowska *et al.* 2007), including two cases of submicroscopic deletion (Soufir *et al.* 2006; Fujii *et al.* 2007). Among these reported cases, four had a nonspecific pattern of malformation as the cases with multiple congenital abnormalities and developmental delay (Ying *et al.* 1982; Farrell *et al.* 1991; Robb *et al.* 1991). Some features of BCNS include age-dependent penetrance, and early diagnosis is important for genetic counseling of patients with the syndrome to prevent harmful exposure to ultraviolet and ionizing radiations that increase the risk of developing basal cell carcinoma (Gorlin & Goltz 1960). Although haploinsufficiency of *PTCH1*, which is mapped on 9q22.3, is associated with BCNS, the diagnosis of BCNS on clinical grounds alone may be challenging, especially during early childhood in patients with monosomy 9q22 (Redon *et al.* 2006).

In the present report, we describe two unrelated patients with some typical features of Gorlin syndrome, including overgrowth and mental retardation, with deletion of 9q22-q31. Furthermore, we determined the boundary of the deletion by fluorescence *in situ* hybridization (FISH) with bacterial artificial chromosome (BAC)

Correspondence: Kenji Kurosawa, MD, PhD, Division of Medical Genetics, Kanagawa Children's Medical Center, 2-138-4 Mutsukawa, Minami-ku, Yokohama 232-8555, Japan. Email: kkurosawa@kcmc.jp

Received August 13, 2008; revised and accepted October 17, 2008.

*These authors contributed equally to this work.

clones. We delineate 9q22 deletion as a recognizable malformation syndrome and review the literature on the reported cases.

MATERIALS AND METHODS

Clinical reports

Patient 1

This boy was the first child of healthy and non-consanguineous parents of normal stature (father's height, 173 cm; mother's height, 159 cm). At the time of the patient's birth, the mother was 26 years of age and the father 27. The patient was born at 41 weeks of gestation after an uncomplicated pregnancy but associated with vacuum-assisted delivery. His birth weight was 3276 g (+0.6 SD), length 51.2 cm (+0.9 SD), and occipitofrontal head circumference (OFC) 34.5 cm (+0.8 SD).

He had difficulties with feeding soon after birth, and he vomited frequently. Because of his characteristic facial appearance and failure to thrive, he was referred to our clinic for detailed examination at 2 months of age. Dysmorphic facial features were present, including apparent strabismus, epicanthic folds, and small mouth with thin upper lip. At 13 months of age, his weight, length, and OFC were 10.82 kg (+1.2 SD), 80.0 cm (+1.6 SD), and 49.8 cm (+2.1 SD), respectively, which represented mild overgrowth, especially macrocephaly. Global developmental delay and speech disturbance were recorded. He began to sit without support at 13 months and walked unassisted at 3 years. Speech and language therapy, and psychomotoric as well as psychomobility training were proposed in early childhood. At 1 and 3 years of age, he had fever-unrelated generalized tonic and clonic convulsions. Carbamazepine treatment was initiated according to the findings of electroencephalogram (EEG) showing multiple focal seizure patterns. Brain computed tomography (CT) showed mild dilatation of the ventricle system and calcification of the falx cerebri. At 3 years of age, he underwent surgery for bilateral strabismus. He attended a special class at a regular school by 7 years of age. At 11 years of age, seizure attacks reappeared. Treatment with valproic acid in addition to carbamazepine was attempted, but seizures recurred. Brain CT and magnetic resonance imaging (MRI) at 12 years of age showed a tumor mass measuring 1.5-cm in diameter in the right frontal cortex (Fig. 1A,B). He underwent right frontal craniotomy and removal of the mass lesion. The pathological diagnosis was ganglioglioma with desmoplasia (World Health Organization grading system, class 1) (Fig. 1C). After the surgery, seizures were improved. Postoperative radiation therapy was avoided because total excision of the tumor was successfully performed and there is no indication of radiation therapy for ganglioglioma. On clinical reexamination at 12 years of age, his height was 140 cm (−1.1SD), weight 37.3 kg (−0.4SD), and OFC 56.3 cm (+1.7 SD). He had some manifestation of BCNS, such as palmar and plantar pits, rib anomalies, pigmented nevi identified on the face, and odontogenic keratocysts. He could speak only a few words, but could not attain toilet control. Overfriendliness and attention deficiency were noted as his behavioral characteristics.

Patient 2

This patient is a 23-year-old male with severe mental retardation and multiple congenital anomalies, including trigonocephaly, cleft lip and palate, and double urethra (Fig. 2A), as well as hyperthyroidism caused by functional thyroid tumor. He was the first child of unrelated parents of normal stature. At the time of birth, the father was 33 years of age and the mother 27. He was born after an uncomplicated pregnancy and uneventful delivery at 41 weeks of gestation. His birth weight was 4222 g (+2.5 SD), height 55 cm (+3.0 SD), and OFC 36.5 cm (+2.1 SD). He was referred to our clinic for poor feeding and facial abnormalities involving cleft lip and palate, hypertelorism, and macrocephaly. He underwent surgical correction of sagittal and metopic craniosynostosis at 6 months of age and cleft lip and palate at 7 months of age. At 3 years of age, he had recurrent episodes of seizures. Additional seizures and further EEG abnormalities led to treatment with phenobarbital. Postnatal overgrowth continued with weight 17.2 kg (+2.6 SD),

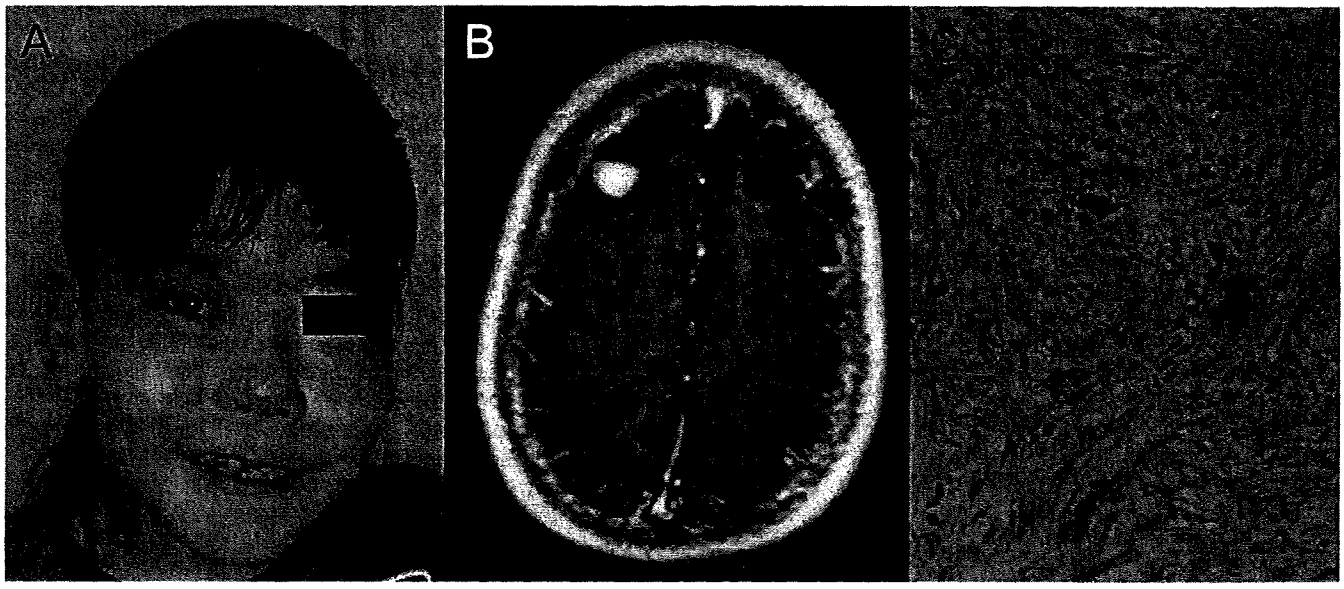

Fig. 1 (A) Facial appearance of patient 1 at 12 years of age. (B) Brain magnetic resonance imaging of the tumor. (C) Photomicrograph of a specimen from the tumor showed that the tumor was composed of neoplastic neuronal or ganglion-like cells and astrocytic cells with varying cell populations.

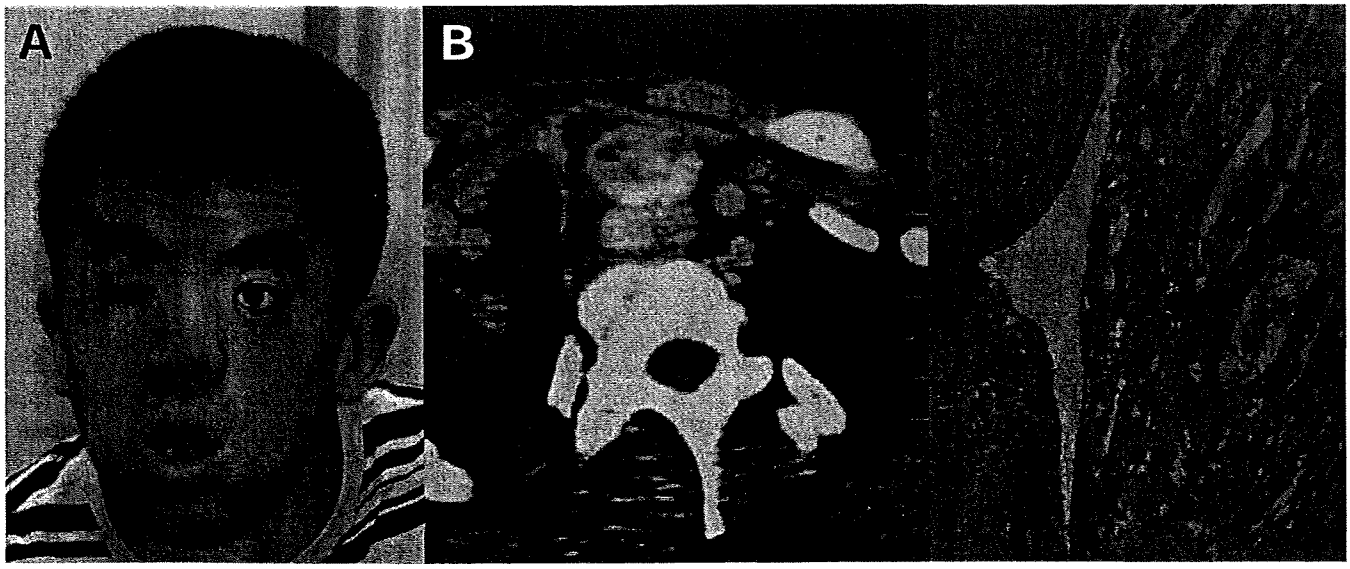

Fig. 2 (A) Facial appearance of patient 2 at 22 years of age. (B) Cervical computed tomography of the tumor in the thyroid gland. (C) Photomicrograph of a specimen from the lobected thyroid gland showed follicular carcinoma with a focus of vascular invasion within the capsule.

length 99.4 cm (+1.9 SD), and OFC 53.2 cm (+2.6 SD) at 3 years of age. He had severe developmental delays, including an intellectual quotient score of 40 at 3 years of age. He began to walk without support at 2.5 years of age and presented behavioral difficulties with hyperactivity and attention deficiency. He attended a school for children with special needs at 7 years of age. At 14 years of age, he was noted to have bilateral maxillary and mandibular multiple odontogenic keratocysts, which were removed by repeat operative procedures. At 16 years of age, he had retinal detachment of the right eyeball, followed by cataract, iris adhesion, and vascularization of unknown injury. Cataract and severe glaucoma associated with hyphemia caused atrophy of his right eyeball. At 16 years of age, hyperthyroidism was detected during regular care examination. Functional nodular goiter diagnosed in laboratory investigation, cervical CT, and ultrasound examination of the thyroid gland was treated by left lobectomy of the thyroid gland (Fig. 2B). The pathological diagnosis was follicular adenocarcinoma without involvement of the attached lymph nodes (Fig. 2C). Obsessive behavior, overfriendliness to strangers, and attention deficit-associated hyperactivity were noted as his behavioral characteristics, which were similar to those of patient 1.

Cytogenetic and FISH analysis

Cytogenetic analyses of chromosomes were performed according to standard protocols. The karyotype was described according to the International System for Human Cytogenetic Nomenclature (ISCN 2005) (Shaffer & Tommerup 2005).

FISH analysis was carried out using BAC clones that were selected by The UCSC Human Genome Browser in March 2006 Assembly (http://genome.ucsc.edu/). All DNA were labeled by nick translation according to the manufacturer's instructions (Nick Translation Mix; Roche Diagnostics, Basel, Switzerland). Centromere probe for chromosome 9 (CEP 9; Vysis, Downer's Grove, IL, USA) were used to confirm chromosome 9. Hybridization, post-hybridization washing and counterstaining were performed as standard procedures. Slides were analyzed using completely motorized epifluorescence microscope (Leica DMRXA2) equipped with CCD camera. Both the camera and microscope were controlled with Leica CW4000 M-FISH software (Leica Microsystems Imaging Solutions, Cambridge, UK).

Written informed consent was obtained from the parents of the patients participating in this study in accordance with the Kanagawa Children's Medical Center Review Board and Ethics Committee.

RESULTS

Conventional cytogenetic analysis by GTG banding on peripheral blood lymphocytes of the patients revealed interstitial deletions of long arm of chromosome 9 in all metaphases. Both sets of parents of patients 1 and 2 had normal karyotypes. The high resolution chromosome analysis showed the karyotype as 46,XY,del(9)(q21.33q22.33)dn in patient 1, and 46,XY,del(9)(q21.33q31.1)dn in patient 2 (Fig. 3).

We further applied molecular cytogenetic techniques using BAC clones to characterize the size of the deletions. The results of these analyses on both patients are summarized in Table 1. In both patients, the centromeric deletion breakpoints were common within chromosomal band 9q21.33 but different regions between RP11-637F3 and RP11-65B23 in patient 1 and between RP11-736H14 and RP11-479K13 in patient 2. The telomeric deletion breakpoints were also common within 9q31.1 but different regions between RP11-368M13 and RP11-351F21 in patient 1 and between RP11-82L2 and RP11-217O12 in patient 2. These analyses established 9q deletions to be located between 15.33 and 16.04 Mb in patient 1 and between 18.08 and 18.54 Mb in patient 2. These results indicate that 97 and 105 RefSeq genes are deleted in patients 1 and 2 respectively.

DISCUSSION

We report two unrelated male patients with de novo 9q21.33-q31.1 deletions, who had multiple congenital anomalies associated with BCNS. To date, more than 19 patients with interstitial deletion of 9q involving chromosomal band q22.3, which includes the *PTCH1*

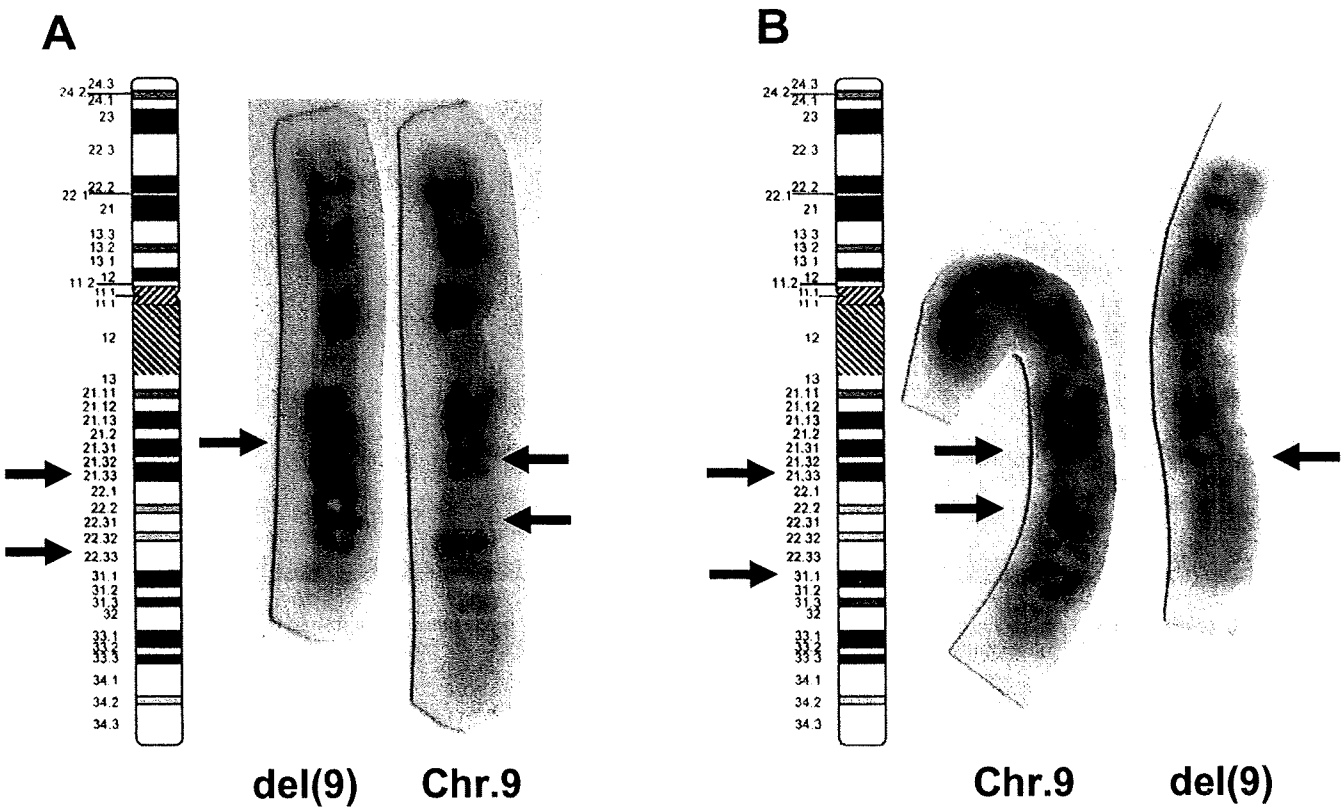

Fig. 3 Partial karyotype showing del(9)(q21.33q22.33) by high resolution banding of a 700-band level in patient 1 (A), and del(9)(q21.33q31.1) in patient 2 (B). The arrows indicate the breakpoints recognized by GTG in the first analysis. The breakpoints of patient 1 were revised as del(9)(q21.33q31.1) according to the results of fluorescence *in situ* hybridization (FISH) analysis.

gene, have been reported. Thus far, only 11 cases with some clinical features common to BCNS associated with 9q deletion have been reported in the published work (Shimkets *et al.* 1996; Olivieri *et al.* 2003; Midro *et al.* 2004; Boonen *et al.* 2005; Chen *et al.* 2006; Redon *et al.* 2006; Fujii *et al.* 2007; Nowakowska *et al.* 2007) (Table 2). Even though the major features of BCNS are also observed among these patients in the same proportion, the clinical manifestations, including mental retardation and dysmorphic features, are inconsistent with the classical phenotypes of BCNS patients. Seizures or epilepsy was found in three (27%) of the 11 cases with large deletion, but only in 6% of the classical cases with BCNS. Both our patients had epilepsy from infancy, which was well-controlled with a single antiepileptic drug. Severe mental retardation is also common in patients with large deletion. Our present cases together with several previously reported cases indicated that the large deletions of 9q involving the critical BCNS regions are responsible for the severe neurological findings when compared with the BCNS patients.

Both our patients had characteristic facial appearance including macrocephaly and small mouth, and a heavy birth weight. They also had characteristic behavior that included hyperactivity and overfriendliness. Large for gestational age is reported in eight of 12 cases with 9q22.3 deletion (Table 2). Redon *et al.* (2006) reported two patients with 6.5 Mb interstitial microdeletions at 9q22.32-q22.33, who had macrocephaly, overgrowth and trigonocephaly. Both these patients had mental retardation, hyperactivity, and distinctive facial appearance. These characteristics are common to our present cases. Redon *et al.* (2006) suggested that the interstitial microdeletion of 9q22.3 is a novel cause of overgrowth and mental retardation and proposed that this unique association is a newly recognized overgrowth syndrome. In addition to the characteristic physical findings and hyperactivity that were recognized as the manifestation of the syndrome, we observed a characteristic trait of obsessive behavior and overfriendliness to strangers in our patients. This distinctive behavior is not described in previous reports. Further studies on cases with 9q deletion are needed to characterize the behavior as a manifestation of the syndrome.

Careful physical evaluation and long-term follow-up is important for the management of patients with BCNS. Regular surveillance involves neurological, dermatological, and dental examinations (Kimonis *et al.* 1997). This is also the case for patients with 9q22.3 deletion associated with BCNS. Except for jaw cysts and basal cell carcinomas (BCC), there was only one case with development of tumor (ameloblastoma) in the previous reports on large deletion of 9q22 (Shimkets *et al.* 1996). We described brain tumor of ganglioblastoma in patient 1 at 13 years of age and adenocarcinoma in the thyroid gland in patient 2 at 22 years of age. In previous reports, because most of the patients with large deletion of 9q22 are below the age of puberty, underestimation of developing tumors is caused by age-dependent penetrance. On the basis of findings in both our patients, it may be hypothesized that the incidence of development of non-BCC tumors is increasing in patients with large deletion of 9q22 associated with BCNS. Further analysis based on long-term follow-up in these patients is important to delineate the syndrome.

Table 1 Fluorescence *in situ* hybridization (FISH) analysis of breakpoints of the deletion on 9q

BAC clones	Chromosome position (distance from 9pter)	Locus	FISH Results Patient 1	Patient 2
RP11-14C18	87 044 608–87 076 587	q21.33	+	+
RP11-293H6	87 101 188–87 266 879	q21.33	+	+
RP11-736H14	87 392 333–87 570 805	q21.33	+	+
RP11-479K13	87 748 255–87 943 468	q21.33	+	del
RP11-164I3	87 988 843–88 174 408	q21.33	+	del
RP11-41K9	88 892 061–88 892 608	q21.33	+	del
RP11-637F3	89 010 177–89 174 385	q21.33	+	del
RP11-65B23	89 444 561–89 614 800	q21.33	del	del
RP11-350G13	90 032 616–90 147 035	q22.1	del	del
RP11-105E2	90 942 479–91 103 543	q22.1–q22.2	del	del
RP11-111J11	91 822 575–91 973 719	q22.2	del	del
RP11-926C20	92 846 239–93 049 991	q22.2–q22.31	del	del
RP11-19J3	94 281 893–94 449 626	q22.31	del	del
RP11-30L4	95 248 566–95 419 410	q22.31	del	del
RP11-2B6	95 889 087–96 054 676	q22.32	del	del
RP11-163C13	97 184 103–97 330 313	q22.32	del	del
RP11-172F4	98 190 057–98 329 174	q22.32–q22.33	del	del
RP11-79A20	98 762 633–98 903 524	q22.33	del	del
RP11-404F11	99 822 932–100 024 231	q22.33	del	del
RP11-506A11	100 825 142–101 031 242	q22.33	del	del
RP11-163K8	101 093 656–101 238 992	q22.33	del	del
RP11-715H1	102 540 777–102 739 074	q31.1	del	del
RP11-54O6	102 696 685–102 869 119	q31.1	del	del
RP11-403A22	103 307 717–103 481 660	q31.1	del	del
RP11-769C21	103 340 520–103 494 438	q31.1	del	del
RP11-644J15	103 515 950–103 706 199	q31.1	del	del
RP11-368M13	104 588 044–104 775 543	q31.1	del	del
RP11-351F21	105 215 416–105 397 660	q31.1	+	del
RP11-454A13	105 789 523–106 004 558	q31.1	+	del
RP11-82L2	105 828 450–105 937 270	q31.1	+	del
RP11-217O12	106 115 003–106 283 618	q31.1	+	+
RP11-240N17	106 175 407–106 335 743	q31.1	+	+
RP11-624P12	107 280 973–107 441 782	q31.2	+	+

BAC, bacterial artificial chromosome.

We determined the deletion breakpoints by FISH using BAC clones mapped on the critical regions in both our patients. The proximal and distal breakpoints were different in both patients. Redon *et al.* (2006) demonstrated that two of their patients with matched phenotypic features had very similar deletions of 6.5 Mb. However, the strict breakpoints and nature of the events leading to the deletions were different between the patients. Fujii *et al.* (2007) investigated three patients using high resolution oligonucleotide microarrays and demonstrated the mechanisms of deletions by determining the junction sequence. As shown in Table 2, the size and breakpoints of deletions varied for each reported case. According to the size and range of deletion, these cases are roughly classified into three groups: a group with a comparatively large size deletion (q21.3-q31), a group with a slightly smaller deletion (q22.3-q31), and a group with the smallest deletion (around q22.3). Except for patient 3 reported by Fujii *et al.* (2007), there appears to be no genotype–phenotype correlation with the chromosomal deletions in the three groups, but it is possible to make predictions about the critical region for the deletion syndrome involving 9q22 responsible for the distinct facial appearance, overgrowth, characteristic behavior, and clinical severity for development and neoplastic features. The common region deleted in these patients encompasses more than 40 RefSeq genes. Overgrowth, especially of prenatal onset, is one of the most prominent features observed in these patients. These data suggest that a growth suppressor gene can be included within the critical region. More patients with 9q22

Table 2 Clinical features in the reported cases with basal cell nevus syndrome (BCNS) associated with 9q deletions

Clinical sings	Frequency in BCNS patients (%) (Farndon 2005)	Present study		Shimkets *et al.* (1996)		Olivieri *et al.* (2003)	Midro *et al.* (2004)	Boonen *et al.* (2005)	Chen *et al.* (2006)	Redon *et al.* (2006)		Fujii *et al.* (2007)			Nowakowska *et al.* (2007)
		Patient 1	Patient 2	Patient 1	Patient 2					Patient 1	Patient 2	Patient 1†	Patient 2	Patient 3	
Age (year)		13	24	15	26	4	12	21	5 M	5	8	12	8	10	12
Sex		Male	Male	Female	Female	Male	Female	Male	Male	Male	Male	Male	Male	Male	Female
Proximal site of breakpoints		q21.33		q22.1	q21.3	q22.31	q22.32	q21.3	q22.3	q22.32		q21.31	q21.2	q22.32	q22.1
Distal site of breakpoints		q31.1		q22.3	q31.1	q31.2	q33.2	q31	q31.3	q22.33		q22.31	q33.1	q22.32	q22.32
Size of deletion (megabases)		15.33–16.04	18.08–18.54	9.8–16.1	17.3–	12.2–19.8		15.3–15.6	12	6.5		11	5.3	0.165	7.7
Overgrowth		+	+	–	–	–	–	NI	+	+	+	NI	NI	NI	NI
Birth weight (g)		3276	4222	NI	NI	3340	3800	3240	4000	4540	5070	3940	NI	NI	3850
Macrocephaly	97	+	+	+	+	+	–	+	+	+	+	+	+	+	+
Mental retardation	3	Severe	Severe	+	+	Severe	Moderate	Mild	NI	Severe	Severe	Severe	Severe	–	Severe
Seizures	6	+	+	–	–	–	–	–	–	–	+	+	+	–	–
Jaw cysts	51	+	+	–	+	–	–	+	–	–	–	+	–	+	+
Palmer/plantar pits	65–80	+	+	–	–	+	–	–	–	–	–	+	+	–	–
Ectopic calcification	40–100	+	–	–	–	–	–	+	–	–	–	+	–	+	–
Skeletal anomalies	~97	+	+	+	+	+	+	+	+	+	+	+	+	+	+
Neoplasms	14–92	Ganglioglioma	Adenocarcinoma in thyroid gland	–	Ameloblastoma	–	BCC	BCC	–	–	–	BCC	–	–	–

†This patient was already reported by Sasaki *et al.* (2000).
BCC, basal cell carcinoma; NI, no information.

deletions characterized by molecular analysis are needed to determine the gene for the recognizable syndrome.

In summary, we have described two patients with deletion of 9q21.33-q31.1 who presented with similar manifestations, including severe mental retardation, prenatal onset overgrowth, distinct facial features, and characteristic behaviors and personality. Although the size and breakpoints were different, these clinical features are common to patients with 9q22 deletion associated with BCNS. Delineation of the 9q22 deletions and further consideration of the genes responsible for the characteristic manifestations may provide insight into the newly recognized deletion syndrome.

ACKNOWLEDGMENTS

This research was supported in part by Grants-in-Aid for Cancer Research from Kanagawa Prefecture, Japan, and the Research Grant (15B-4, 18A-5) for Nervous and Mental Disorders from the Ministry of Health, Labour and Welfare, Japan (K.K.). The authors are grateful to Dr Hiroyuki Ida (Tokyo Jikei University) for his valuable comments and SRL (Special Reference Laboratories Inc., Tokyo, Japan) for technical support. The authors also wish to thank the patients and their families for contributing to this study.

REFERENCES

Boonen SE, Stahl D, Kreiborg S *et al.* (2005) Delineation of an interstitial 9q22 deletion in basal cell nevus syndrome. *Am J Med Genet* **132A**: 324–328.

Chen C-P, Lin S-P, Wang T-H, Chen W-J, Chen M, Wang W (2006) Perinatal findings and molecular cytogenetic analysis of de novo interstitial deletion of 9q (9q22.3→q31.3) associated with Gorlin syndrome. *Prenat Diagn* **26**: 725–729.

Evans DGR, Farndon PA, Burnell LD, Gattamaneni HR, Birch JM (1991) The incidence of Gorlin syndrome in 173 consecutive cases of medulloblastoma. *Br J Cancer* **64**: 959–961.

Farndon F (2005) Gorlin syndrome (Nevoid basal cell carcinoma syndrome). In: Cassidy SB, Allanson JE (eds). *Management of Genetic Syndromes*, 2nd edn. Wiley-Liss, Hoboken, NJ, pp. 265–278.

Farrell SA, Siegel-Bartelt J, Teshima I (1991) Patients with deletions of 9q22q34 do not define a syndrome: Three case reports and a literature review. *Clin Genet* **40**: 207–214.

Fujii K, Ishikawa S, Uchikawa H *et al.* (2007) High-density oligonucleotide array with sub-kilobase resolution reveals breakpoint information of submicroscopic deletions in nevoid basal cell carcinoma syndrome. *Hum Genet* **122**: 459–466.

Gorlin RJ, Goltz RW (1960) Multiple nevoid basal-cell epithelioma, jaw cysts and bifid rib: A syndrome. *New Engl J Med* **262**: 908–912.

Hahn H, Wicking C, Zaphiropulos PG *et al.* (1996) Mutations of the human homolog of Drosophila patched in the nevoid basal cell carcinoma syndrome. *Cell* **85**: 841–851.

Haniffa MA, Leech NS, Lynch LSA, Simpson NB (2004) NBCCS secondary to an interstitial chromosome 9q deletion. *Clin Exp Dermatol* **29**: 542–544.

Johnson RL, Rothman AL, Xie J *et al.* (1996) Human homolog of patched, a candidate gene for the basal cell nevus syndrome. *Science* **272**: 1668–1671.

Kimonis VE, Goldstein AM, Pastakia B *et al.* (1997) Clinical manifestations in 105 persona with nevoid basal cell carcinoma syndrome. *Am J Med Genet* **69**: 299–308.

Kroes HY, Tuerlings JHAM, Hordijk R, Folkers NRP, ten Kate LP (1994) Another patient with an interstitial deletion of chromosome 9: Case report and a review of six cases with del(9)(q22q32). *J Med Genet* **31**: 156–158.

Lindström E, Shimokawa T, Toftgård R, Zaphiropoulos PG (2006) PTCH mutations: Distribution and analyses. *Hum Mutat* **27**: 215–219.

Midro AT, Panasiuk B, Tümer Z *et al.* (2004) Interstitial deletion 9q22.32–q33.2 associated with additional familial translocation t(9;17)(q34.11;p11.2) in a patient with Gorlin-Goltz syndrome and features of nail-patella syndrome. *Am J Med Genet* **124A**: 179–191.

Nowakowska B, Kutkowska-Kazmierczak A, Stankiewicz P *et al.* (2007) A girl with deletion 9q22.1–q22.32 including the *PTCH* and *ROR2* genes identified by genome-wide array-CGH. *Am J Med Genet* **143A**: 1885–1889.

Olivieri C, Maraschio P, Caselli D *et al.* (2003) Interstitial deletion of chromosome 9, int del(9)(9q22.31–q31.2), including the genes causing multiple basal cell nevus syndrome and Robinow/brachydactyly 1 syndrome. *Eur J Pediatr* **162**: 100–103.

Redon R, Baujat G, Sanlaville D *et al.* (2006) Interstitial 9q22.3 microdeletion: Clinical and molecular characterization of a new recognized overgrowth syndrome. *Eur J Hum Genet* **14**: 759–767.

Robb LJ, Vekemans M, Richter A, Meagher-Villemure K, Neilsen K, der Kaloustian VM (1991) Interstitial deletion of the long arm of chromosome 9. *Am J Hum Genet* **49**: 174.

Sasaki K, Yoshimoto T, Nakao T *et al.* (2000) A nevoid basal cell carcinoma syndrome with chromosomal aberration. *No to Hattatsu* **32**: 49–55.

Shaffer LG, Tommerup N (2005) *ISCN 2005: An International System for Human Cytogenetic Nomenclature*. S. Karger, Basel.

Shimkets R, Gailani MR, Siu VM *et al.* (1996) Molecular analysis of chromosome 9q deletions in two Gorlin syndrome patients. *Am J Hum Genet* **59**: 417–422.

Soufir N, Gerard B, Portela M *et al.* (2006) PTCH mutations and deletions in patients with typical nevoid basal cell carcinoma syndrome and in patients with a suspected genetic predisposition to basal cell carcinoma: A French study. *Br J Cancer* **95**: 548–553.

Wicking C, Shanley S, Smyth I *et al.* (1997) Most germ-line mutations in the nevoid basal cell carcinoma syndrome lead to a premature termination of PATCHED protein and no genotype-phenotype correlations are evident. *Am J Hum Genet* **60**: 21–26.

Ying KL, Curry CJR, Rajani KB, Kassal SH, Sparkes RS (1982) *De novo* interstitial deletion in the long arm of chromosome 9: A new chromosome syndrome. *J Med Genet* **19**: 68–76.

Journal of Human Genetics (2009) 54, 304–309

www.nature.com/jhg

ORIGINAL ARTICLE

Molecular karyotyping in 17 patients and mutation screening in 41 patients with Kabuki syndrome

Hideo Kuniba[1,2,14], Koh-ichiro Yoshiura[1,14], Tatsuro Kondoh[2], Hirofumi Ohashi[3,14], Kenji Kurosawa[4], Hidefumi Tonoki[5], Toshiro Nagai[6,14], Nobuhiko Okamoto[7], Mitsuhiro Kato[8], Yoshimitsu Fukushima[9,14], Tadashi Kaname[10,14], Kenji Naritomi[10,14], Tadashi Matsumoto[2], Hiroyuki Moriuchi[2], Tatsuya Kishino[11,14], Akira Kinoshita[1,14], Noriko Miyake[12,14], Naomichi Matsumoto[12,14] and Norio Niikawa[1,13,14]

The Kabuki syndrome (KS, OMIM 147920), also known as the Niikawa–Kuroki syndrome, is a multiple congenital anomaly/mental retardation syndrome characterized by a distinct facial appearance. The cause of KS has been unidentified, even by whole-genome scan with array comparative genomic hybridization (CGH). In recent years, high-resolution oligonucleotide array technologies have enabled us to detect fine copy number alterations. In 17 patients with KS, molecular karyotyping was carried out with GeneChip 250K NspI array (Affymetrix) and Copy Number Analyser for GeneChip (CNAG). It showed seven copy number alterations, three deleted regions and four duplicated regions among the patients, with the exception of registered copy number variants (CNVs). Among the seven loci, only the region of 9q21.11-q21.12 (~1.27 Mb) involved coding genes, namely, transient receptor potential cation channel, subfamily M, member 3 (*TRPM3*), Kruppel-like factor 9 (*KLF9*), structural maintenance of chromosomes protein 5 (*SMC5*) and MAM domain containing 2 (*MAMDC2*). Mutation screening for the genes detected 10 base substitutions consisting of seven single-nucleotide polymorphisms (SNPs) and three silent mutations in 41 patients with KS. Our study could not show the causative genes for KS, but the locus of 9q21.11-q21.12, in association with a cleft palate, may contribute to the manifestation of KS in the patient. As various platforms on oligonucleotide arrays have been developed, higher resolution platforms will need to be applied to search tiny genomic rearrangements in patients with KS.
Journal of Human Genetics (2009) **54**, 304–309; doi:10.1038/jhg.2009.30; published online 3 April 2009

Keywords: Kabuki syndrome; microdeletion; molecular karyotyping; mutation screening; Niikawa–Kuroki syndrome

INTRODUCTION

Kabuki syndrome (KS, OMIM 147920), also known as Niikawa–Kuroki syndrome, is a multiple congenital anomaly/mental retardation (MCA/MR) syndrome characterized by a distinct facial appearance, skeletal abnormalities, joint hypermobility, dermatoglyphic abnormalities, postnatal growth retardation, recurrent otitis media and occasional visceral anomalies.[1,2] The prevalence was estimated to be 1/32 000 in Japan[3] and 1/86 000 in Australia and New Zealand.[4] Although most cases were sporadic, at least 14 familial cases have been reported. It is assumed that KS is an autosomal dominant disorder, considering the equal male-to-female ratio of patients and parent–child transmission pattern in some familial cases.[5]

The cause of KS remains unknown, even though at least 400 patients have been diagnosed in a variety of ethnic groups since 1981.[3–7] Some works have ruled out several loci; for example, 1q32–q41, 8p22–p23.1 and 22q11, as candidates for KS.[8–13] A study of array-based comparative genomic hybridization (CGH) showed a disruption of the *C20orf133(MACROD2)* gene by ~250 kb deletion in a patient with KS,[14] but the following mutation screening for the gene failed to find a pathogenic base change within exons in 19 other patients with KS[14] and in 43 Japanese patients.[15] Another study of array CGH with 0.5–1.2 Mb resolution reported that 2q37 deletions were detected in two patients with Kabuki-like features, but their facial features were not typical for KS.[16] To date, no concordant specific lesion has been

[1]Department of Human Genetics, Nagasaki University Graduate School of Biomedical Sciences, Nagasaki, Japan; [2]Department of Pediatrics, Nagasaki University School of Medicine, Nagasaki, Japan; [3]Division of Medical Genetics, Saitama Children's Medical Center, Iwatsuki, Japan; [4]Division of Medical Genetics, Kanagawa Children's Medical Center, Yokohama, Japan; [5]Department of Pediatrics, Tenshi Hospital, Sapporo, Japan; [6]Department of Pediatrics, Dokkyo University School of Medicine Koshigaya Hospital, Koshigaya, Japan; [7]Department of Planning and Research, Osaka Medical Center and Research Institute for Maternal and Child health, Osaka, Japan; [8]Department of Pediatrics, Yamagata University School of Medicine, Yamagata, Japan; [9]Department of Medical Genetics, Shinshu University School of Medicine, Matsumoto, Japan; [10]Department of Medical Genetics, University of the Ryukyus, Nishihara, Japan; [11]Division of Functional Genomics, Center for Frontier Life Sciences, Nagasaki University, Nagasaki, Japan; [12]Department of Human Genetics, Yokohama City University Graduate School of Medicine, Yokohama, Japan; [13]Research Institute of Personalized Health Sciences, Health Sciences University of Hokkaido, Tobetsu, Japan and [14]Solution Oriented Research for Science and Technology (SORST), Japan Science and Technology Agency (JST), Tokyo, Japan
Correspondence: Dr K-i Yoshiura, Department of Human Genetics, Nagasaki University Graduate School of Biomedical Sciences, Sakamoto 1-12-4, Nagasaki 852-8523, Japan.
E-mail: kyoshi@nagasaki-u.ac.jp
Received 15 January 2009; revised 3 March 2009; accepted 11 March 2009; published online 3 April 2009

found by whole-genome scan with array CGH in a bacterial artificial chromosome (BAC) clone with 0.5–1.5 Mb resolution.[16–18]

Chromosomal aberration analysis by high-resolution oligonucleotide array technologies in recent years, called molecular karyotyping, enables us to detect submicroscopic pathogenic copy number alterations, which were undetectable even by BAC array CGH.[19,20] As not a few MCA/MR syndromes are because of chromosomal copy number aberration, we hypothesize that some sort of microdeletion/microduplication causes KS. Herein, we report the results of molecular karyotyping in 17 patients using GeneChip 250K array and those of mutation screening of candidate genes in 41 patients with KS in Japan.

MATERIALS AND METHODS

Subjects

The subjects for molecular karyotyping consisted of 18 patients (nine girls and nine boys) at entry. The subjects for mutation screening consisted of 41 patients (20 girls and 21 boys), including the aforementioned 18 patients. The diagnoses of KS were confirmed by experts of clinical genetics, although written permission for the use of facial photographs in publications was not obtained. These Japanese patients showed a normal karyotype at a 400-band level, and were earlier reported with no pathogenic genome copy number change by 1.5 Mb-resolution BAC array CGH.[18] Genomic DNA was isolated by the standard method from their peripheral blood leukocytes or in part from their lymphoblastoid cell lines. Experimental procedures were approved by the Committee for the Ethical Issues on Human Genome and Gene Analysis at Nagasaki University.

Molecular karyotyping

DNA oligomicroarray hybridization, using the GeneChip Human Mapping 250K Nsp Array (Affymetrix, Santa Clara, CA, USA), was carried out for 18 patients with KS, following the provided protocol (Affymetrix). Data were analyzed using GTYPE (GeneChip Genotyping Analysis Software) to detect copy number aberration and visualized using CNAG (Copy Number Analyser for GeneChip) version 3.[21] References for non-paired analysis of CNAG were chosen from eight unrelated individuals of HapMap samples from the Affymetrix website (http://www.affymetrix.com/support/). The resolution of this procedure was estimated as ~30–100 kb. CNAG version 3 was linked with the University of California Santa Cruz (UCSC) genome browser (http://genome.ucsc.edu/) assembly May 2004, and then its physical position was referred to the data assembly on March 2006 in the UCSC genome browser after adjustment.

Validation of deletion

Quantitative PCR (qPCR) analysis to validate deletions was run on a Light-Cycler 480 Real-Time PCR System (Roche Diagnostics, Mannheim, Germany) using an intercalating dye, SYTO9 (Molecular probes, OR, USA), which is an alternative to SYBR green I.[22] Absolute quantification was carried out using a second derivative max method. A standard curve of amplification efficiency for each set of primers was generated with a serial dilution of genomic DNA. A corrected gene dosage was given as the ratio of a target gene divided by an internal control gene. The copy number was obtained from a calibration under the assumption that the control genome was diploid.

Target genes of copy number aberration were as follows: *SUMF1* (for patient K9); *MAMDC2* (for patient K16); and *CETN1* (for patient K34). The primer sequences of these genes are available in the online supplementary file. Internal control diploid genes were *OAZ2* and *USP21*. Primer sets of the control genes for genomic DNA were selected from the Real Time PCR Primer Sets website (http://www.realtimeprimers.org/). The control genes were confirmed to have no copy number variants on the Database of Genomic Variants (DGV) updated on 26 June 2008 (http://projects.tcag.ca/variation/). BLAST searches confirmed all primer sequences specific for the gene.

Samples were analyzed in triplicate in a 384-well format in a 10 μl final volume containing about 2 ng genomic DNA, 0.5 μM forward primer, 0.5 μM reverse primer, 0.1 Units TaKaRa ExTaq HS version (TaKaRa, Kyoto, Japan), 1× PCR buffer, 200 μM dNTP and 0.5 μM SYTO9. The amplification conditions consisted of an initial denaturation at 95 °C for 5 min, followed by 45 cycles of

Table 1 Detected genomic copy number aberrations in 17 patients with Kabuki syndrome

Cytoband	*Patient(s) ID*	*CN State*	*Length*	*Physical position*		*Involving gene(s)*	*Concordant loss/gain on DGV*
				Start	*End*		
3p26.3	K7	1	460 kb	1435279	1895554	NR	Variation_8235
3p26.2	K9	1[a]	205 kb	4009368	4214847	*SUMF1*	Variation_8973, 8975, 30169
4q13.2	K23	1[a]	1.26 Mb	66329014	67591611	NR	NR
5q21.2-q21.3	K22	1	281 kb	104301325	104581898	NR	Variation_3568
9q21.11-q21.12	K16	1[a]	1.27 Mb	71760296	73031176	*TRPM3, KLF9, SMC5, MAMDC2*	NR
14q11.2	K5	1	166 kb	19336854	19502641	*OR4N2, OR4K2, OR4K5, OR4K1*	Variation_0376, 7028, 8094, 9234, 9235
15q11.2	K1, K23	1	972 kb	19356830	20329239	*OR4M2, OR4N4, LOC65D137*	Variation_0318, 3070, 8265, 9251, 9254, 9256
18p11.32	K34	1[a]	35 kb	545074	580003	*CETN1*	Variation_5044
20p12.1	K6	1[a]	152 kb	14993412	15145890	*C20orf133 (MACROD2)*[b]	NR
4q12	K5	3	104 kb	54251599	54355281	NR	NR
8q11.21	K7	3	171 kb	50641101	50812548	NR	Variation_2751, 3731, 8601, 37765
10p15.2-p15.1	K5	3	142 kb	3663600	3805292	NR	NR
13q31.1	K6	3	72 kb	82451568	82523728	NR	NR
15q11.2	K7, K9, K12	3	877 kb	19112164	19989036	*CXADRP2, POTEB*	Variation_3070, 3951, 8784, 30670, etc.
15q25.1	K9	3	165 kb	76992181	77156751	*CTSH, RASGRF1*	Variation_3970, 7073
16q21	K13	3	283 kb	58508008	58791285	NR	NR
17q12	K7	3	495 kb	31428390	31923810	*CCL3, CCL4, CCL3L1, CCL3L3, CCL4L1, CCL4L2, TBC1D3B, TBC1D3C, TBC1D3G*	Variation_3142, 4031, 8841, 30824, etc.
22q11.22	K5, K12	3	278 kb	20907806	21186081	*VPREB1, ZNF280B*	Variation_5356, 34540

Abbreviations: CN, copy number; DGV, Database of Genomic Variants; NR, no registration in UCSC genes or DGV.
[a]Validated by quantitative PCR.
[b]Deleted region was within intron 5 of the *C20orf133 (MACROD2)* and did not involve any coding exon.[15]

denaturation at 95 °C for 10 s, annealing at 55 °C for 10 s and extension at 72 °C for 15 s The data were analyzed using LightCycler 480 Basic Software (Roche Diagnostics) and the melting curve was checked to eliminate non-specific products from the reaction.

Mutation screening of candidate genes

Candidate genes, identified within a detected deletion, consisted of four genes: *TRPM3* (NM_001007471 and NM_206946), *KLF9* (NM_001206), *SMC5* (NM_015110) and *MAMDC2* (NM_153267) located at 9q21.12–q21. 11. The entire coding region and splice junctions of the genes were sequenced on an automated sequencer 3130xl (Applied Biosystems, Foster City, CA, USA) using BigDye version 3.1 (Applied Biosystems). Genomic sequences were retrieved from the UCSC genome browser (assembly: March 2006). PCR primers were designed with the assistance of Primer3 (http://frodo.wi.mit.edu/cgi-bin/primer3/primer3.cgi). The primer sequences are available in the online supplementary file. Resultant electropherograms were aligned using ATGC version 3.0 (Software Development, Tokyo, Japan) and inspected visually to find DNA alterations.

In silico analysis

Relations among deleted genes were assessed using online software, PANTHER (Protein Analysis Through Evolutionary Relationships, http://www.pantherdb.org), to determine whether the genes involve some developmental pathway or biological process.[23] The novel synonymous base substitutions found in the mutation screening were examined for their potential activation of the cryptic splice site by comparison between wild-type allele and mutated allele using the GeneSplicer program (http://www.cbcb.umd.edu/software/GeneSplicer/gene_spl.shtml).

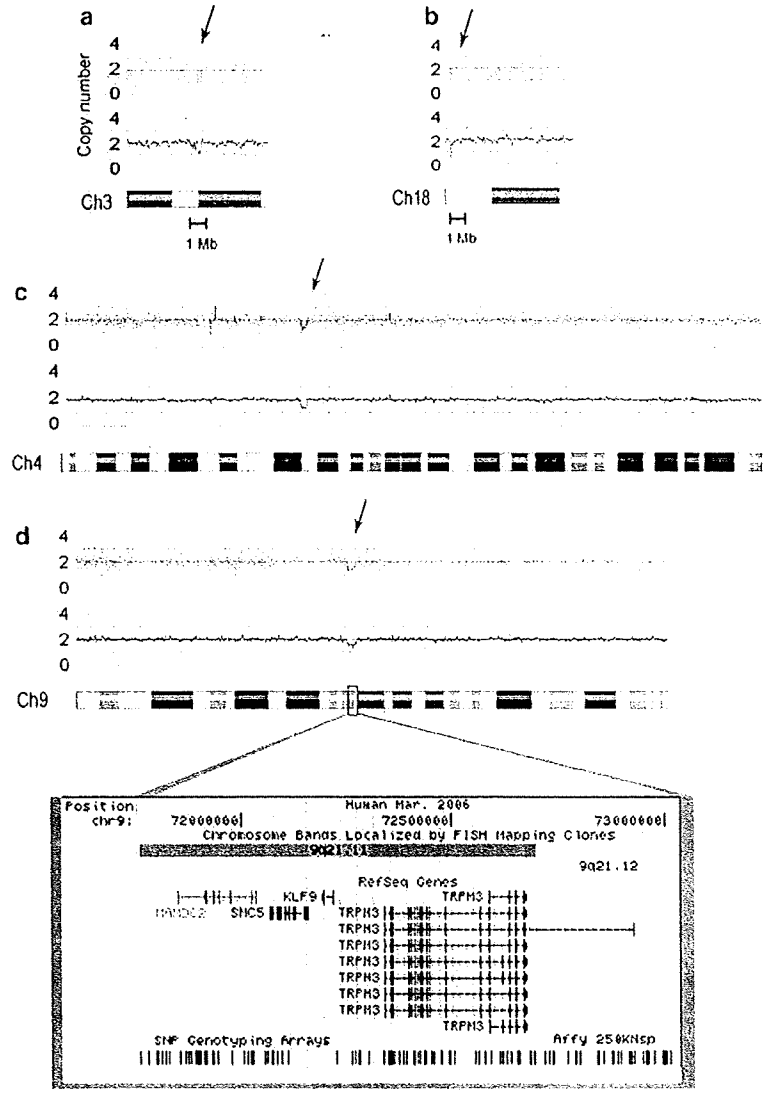

Figure 1 Chromosome view of Copy Number Analyser for GeneChip (CNAG) analysis. Each dots represent fluorescent intensity on each single-nucleotide polymorphisms (SNP) probe of GeneChip 250K NspI array (Affymetrix). Solid lines indicate copy number analyzed with CNAG. Arrows show detected deletions. (**a**) Chromosome (Ch) 3 of patient K9, ~205 kb deletion in 3p26.2 involving an exon of *SUMF1*gene. (**b**) Chromosome 18 of patient K34, ~35 kb deletion in 18p11.32, containing the *CETN1* gene. (**c**) Chromosome 4 of patient K23, ~1.26 Mb deletion in 4q13.2, not involving any known gene. (**d**) Chromosome 9 of patient K16, ~1.27 Mb deletion in 9q21.11–q21.12, harboring four genes: *TRPM3*, *KLF9*, *SMC5* and *MAMDC2*. The University of California Santa Cruz genome browser denotes the cytobands, genes and probe setting of Affymetrix 250K NspI array within the region. No copy number variation was registered here in the Database of Genomic Variants updated 26 June 2008. FISH, fluorescent *in situ* hybridization.

RESULTS

Molecular karyotyping and validation of deletion

The entries of molecular karyotyping were 18 patients with KS (K1, K3, K5, K6, K7, K8, K9, K11, K12, K13, K16, K18, K20, K21, K22, K23, K34 and K38). We eliminated the data of patient K3 from copy number analysis, because it showed low quality data; that is, a single-nucleotide polymorphism (SNP) call rate of 82.51% and a quality control performance detection rate of 74.09%, probably because of DNA degradation during long-term storage. The other patients showed high call rates, enough for copy number analysis (SNP call rate of 90.07–97.72% and detection rate of 91.52–99.77%). We identified nine deleted regions, the lengths of which were between ~35 kb and ~1.27 Mb, and nine duplicated regions, of lengths between ~72 and ~495 kb, in the 17 patients analyzed (Table 1). As for the nine duplications detected, five of them were concordant to several observed gains in DGV, and four of them in each patient did not contain any known genes.

It is interesting that the deleted region of 9q21.11–q21.12 (~1.27 Mb in patient K16), which had not been registered in DGV, harbored four known genes: transient receptor potential cation channel, subfamily M, member 3 (*TRPM3*), Kruppel-like factor 9 (*KLF9*), structural maintenance of chromosomes protein 5 (*SMC5*) and MAM domain containing 2 (*MAMDC2*) (Figure 1d). The deletion of 3p26.2 (~205 kb in patient K9, Figure 1a) had involved a non-coding exon of the *SUMF1* gene. The deletion of 18p11.32 (~35 kb in patient K34, Figure 1b) containing the *CETN1* gene had one registration in DGV as Variation_5044, which described only one observed loss and 14 observed gains in 95 individuals. The deletion of 4q13.2 (~1.26 Mb in patient K23, Figure 1c) and 20p12.1 (~152 kb in patient K6) did not carry any coding exon of any gene. The regions of 14q11.2 (~116 kb in patient K5) and 15q11.2 (~972 kb in patient K1 and K23) were non-pathological deletions with as many registrations as observed losses in DGV.

To validate the deletion of the detected region, we confirmed the loss of heterozygosities of the SNP probes present there using GTYPE (data not shown) and carried out qPCR. The regions of *SUMF1* on 3p26.2 (for patient K9) and of *MAMDC2* on 9q21.11–q21.12 (for patient K16) had one copy in each patient compared with those in unaffected individuals (Figure 2). The deletion of *CETN1* on 18p11.32 (for patient K34) was inherited from his unaffected mother. As samples from the parents of patient K16 were unavailable, it was not possible to examine whether the deletion of 9q21 was *de novo*. But the deletion was not found in 95 normal Japanese individuals using qPCR (data not shown).

As a consequence of this copy number analysis, we considered the next four genes as candidate genes for KS: *TRPM3*, *KLF9*, *SMC5* and *MAMDC2*.

Mutation screening and *in silico* analysis

Table 2 shows the results from mutation screening of the four candidate genes in 41 patients with KS. Ten base substitutions were found in the 41 patients, consisting of six registered SNPs, one unregistered SNP and three silent mutations. In addition, *SUMF1* (NM_182760) and *CETN1* (NM_004066) were also screened, but no mutations were detected (data not shown).

We checked the three silent mutations for splice site alteration using the GeneSplicer program, but no activation of the cryptic splice site was predicted. Although PANTHER classification of the four candidate genes did not show significant correlation for biological processes or pathway because of its small scale in number, some genes associated with developmental biology; that is, DNA repair (*SMC5*) and mRNA transcription regulation (*KLF9*).

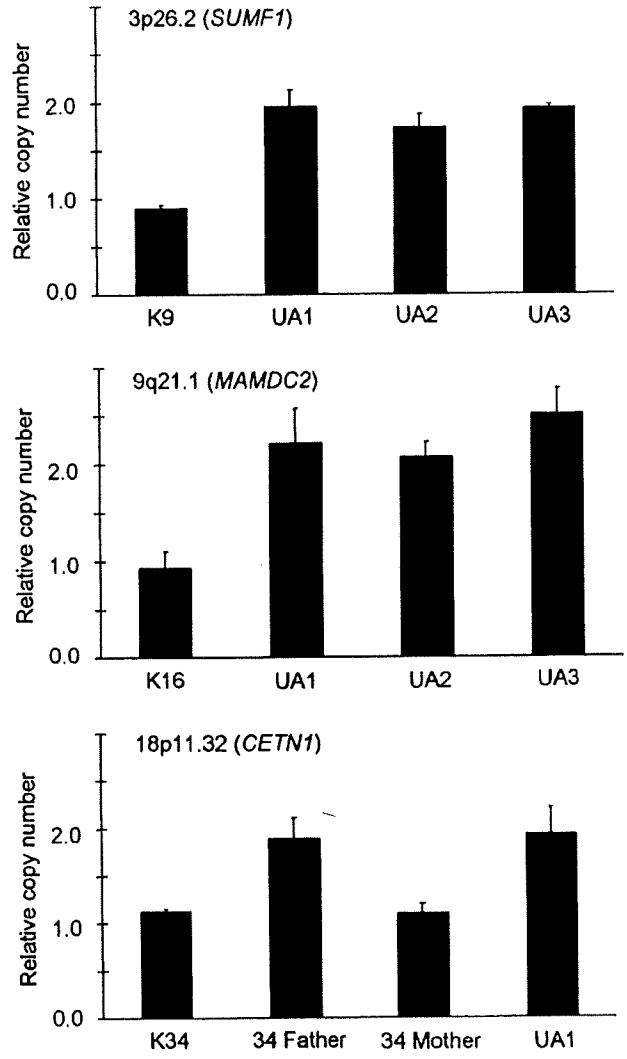

Figure 2 Validation of deletion with quantitative PCR (qPCR). qPCR confirmed a loss of one copy in each patient: *SUMF1* at 3p26.2 for patient K9; *MAMDC2* at 9q21.1 for patient K16; *CETN1* at 18p11.32 for patient K34. The deletion of patient K34 was inherited from his unaffected mother. UA, unaffected individual. Error bars, s.d.

DISCUSSION

We used high-resolution oligonucleotide array of GeneChip 250K NspI with a resolution of 30–100 kb and tried to find causative deletions or mutated genes for KS. Our molecular analysis did not strongly identify the causative gene for KS, but we identified a locus that possibly contributed to KS.

The deletion in patient K16, with a length of ~1.27 Mb at 9q21.11–q21.12, harbored four known genes: *TRPM3*, *KLF9*, *SMC5* and *MAMDC2* (Figure 1d). Unfortunately, her parents' DNAs were unavailable, but the region is unlikely to be a copy number variant (CNV) because it has not been known as CNV in DGV; moreover, the deletion was not found in 95 normal Japanese individuals using qPCR.

As mutation screening in the 41 patients with KS showed no pathogenic base substitution in these genes, we cannot state that